

Targeting the NF- κ B p65/Bcl-2 signaling pathway in hepatic cellular carcinoma using radiation assisted synthesis of zinc nanoparticles coated with naturally isolated gallic acid

Omayma A.R. AboZaid^a, Mostafa A. Abdel-Maksoud^b, Ibrahim A. Saleh^c, Mohamed A. El-Tayeb^b, Sawsan M. EL-sonbaty^d, Faten E. Shoker^a, Maha A. Salem^e, Ayat M. Emad^f, Samson Mani^{g,h}, Arunagiri Kuha Deva Magendhra Rao^h, Mohamed A. Mamdouhⁱ, Mohamed H. Kotob^{j,k}, Mohammed Aufy^{j,*}, Ahmad S. Kodous^{h,l,**}

^a Department of Biochemistry, Faculty of Veterinary Medicine, Moshtohor, Benha University, Egypt

^b Botany and Microbiology department- College of Science- King Saud University, Saudi Arabia

^c Faculty of Science, Zarqa University, Zarqa 13110, Jordan

^d Radiation Microbiology Department, National Center for Radiation Research & Technology (NCRRT), Egyptian Atomic-Energy Authority (EAEA), Egypt

^e Pharmacology and Toxicology Department, Faculty of Pharmacy, Modern University for Technology and Information, Egypt

^f Pharmacognosy Department, Faculty of Pharmacy, October 6 University, Sixth of October City, Giza 12585, Egypt

^g Department of Research, Rajiv Gandhi Cancer Institute, and Research Centre, Sector 5, Rohini, Delhi 110085, India

^h Department of Molecular Oncology, Cancer Institute (WIA), 38, Sardar Patel Road, P.O. Box 600036, Chennai, Tamilnadu, India

ⁱ Department of Pharmaceutics and Industrial Pharmacy, Faculty of Pharmacy, October 6 University, 6th of October City, Giza 12585, Egypt

^j Department of Pharmaceutical Sciences, Division of Pharmacology and Toxicology, University of Vienna, Vienna, Austria

^k Department of Pathology, Faculty of Veterinary Medicine, Assiut University, Assiut, Egypt

^l Radiation Biology department, National Center for Radiation Research & Technology (NCRRT), Egyptian Atomic-Energy Authority (EAEA), Egypt

ARTICLE INFO

Keywords:

Hepatic carcinoma
Pomegranate peel
Gallic acid
Radiation
Zn-GANPs
NF- κ B p65
Bcl-2
G2/M
TGF- β 1

ABSTRACT

Purpose: Oral diethylnitrosamine (DEN) is a known hepatocarcinogen that damages the liver and causes cancer. DEN damages the liver through reactive oxygen species-mediated inflammation and biological process regulation.

Materials and methods: Gallic acid-coated zinc oxide nanoparticles (Zn-GANPs) were made from zinc oxide (ZnO) synthesized by irradiation dose of 50 kGy utilizing a Co-60 γ -ray source chamber with a dose rate of 0.83 kGy/h and gallic acid from pomegranate peel. UV-visible (UV) spectrophotometry verified Zn-GANP synthesis. TEM, DLS, and FTIR were utilized to investigate ZnO-NPs' characteristics.

Rats were orally exposed to DEN for 8 weeks at 20 mg/kg five times per week, followed by intraperitoneal injection of Zn-GANPs at 20 mg/kg for 5 weeks. Using oxidative stress, anti-inflammatory, liver function, histologic, apoptotic, and cell cycle parameters for evaluating Zn-GANPs treatment.

Results: DEN exposure elevated inflammatory markers (AFP and NF- κ B p65), transaminases (AST, ALT), γ -GT, globulin, and total bilirubin, with reduced protein and albumin levels. It also increased MDA levels, oxidative liver cell damage, and Bcl-2, while decreasing caspase-3 and antioxidants like GSH, and CAT. Zn-GANPs significantly mitigated these effects and lowered lipid peroxidation, AST, ALT, and γ -GT levels, significantly increased CAT and GSH levels ($p < 0.05$). Zn-GANPs caused S and G2/M cell cycle arrest and G0/G1 apoptosis. These results were associated with higher caspase-3 levels and lower Bcl-2 and TGF- β 1 levels. Zn-GANPs enhance and restore the histology and ultrastructure of the liver in DEN-induced rats.

Conclusion: The data imply that Zn-GANPs may prevent and treat DEN-induced liver damage and carcinogenesis.

* Corresponding author.

** Corresponding author at: Department of Molecular Oncology, Cancer Institute (WIA), 38, Sardar Patel Road, P.O. Box 600036, Chennai, Tamilnadu, India.

E-mail addresses: Mohammed.aufy@univie.ac.at (M. Aufy), ahmadkmp11@gmail.com (A.S. Kodous).

<https://doi.org/10.1016/j.bioph.2024.116274>

Received 11 December 2023; Received in revised form 1 February 2024; Accepted 13 February 2024

Available online 15 February 2024

0753-3322/© 2024 The Author(s). Published by Elsevier Masson SAS. This is an open access article under the CC BY-NC-ND license (<http://creativecommons.org/licenses/by-nc-nd/4.0/>).

1. Introduction

Liver cancer is globally recognized as the sixth most frequently diagnosed cancer, with approximately 841,000 new cases and 782,000 annual fatalities. Incidence and mortality rates are notably higher in males, surpassing those in females by a factor of 2–3 [1]. Hepatocellular carcinoma (HCC) is typically the consequence of cirrhosis and is a major contributor to cancer-related mortality, ranking as the second leading cause of such deaths. [2]. One of the HCC carcinogens is diethylnitrosamine (DEN), a nitrosamine-class chemical environmental carcinogen that contaminates humans via the food chain. DEN is generated endogenously and is present in occupational environments, tobacco smoke, processed meat, alcohol, agricultural chemicals, cosmetics, and pharmaceuticals. It also comes from medication metabolism [3]. The major challenge in HCC therapy is targeting.

Nanotechnology has created multifunctional nanoparticles for targeted and effective HCC therapy [4]. Nanotechnology involves use of nanometer-scale materials (1–100 nm) [5] or nanoparticles which deliver anticancer and other medicines to tumor locations without harming normal tissues [5].

Zinc oxide (ZnO) nanoparticles are one type of possible anticancer nanoparticles that promote apoptosis in human cancer cells by increasing reactive oxygen species (ROS) in malignant T cells compare to normal T cells [6]. It has shown that ZnO NPs selectively kill hepatic cancer cells [7]. Zinc ions help make "zinc fingers," which are DNA-binding sequences that are found in structural and regulatory proteins like transcription factors [8]. Over two billion individuals worldwide suffer from zinc insufficiency [9]. The blood zinc level of many cancer patients, notably lung, breast, liver, head, and neck cancer patients, is low [10]. Due to its many roles, this element may have a key role in preventing cancer and therefore low cytotoxic effect [11].

Furthermore, pomegranate (*Punica granatum* L.), a member of the Punicaceae family, stands as a nutrient-dense food source renowned for its abundance of phenolic compounds and gallic acid (GA) [12]. It was revealed that pomegranate juices display significantly high antioxidant activity, surpassing the antioxidant capacity of green tea and red wine by nearly threefold [13]. GA, a polyhydroxylphenolic compound, is found in pomegranate, numerous fruits, plants, and food sources. It has demonstrated antiviral, antibacterial, anti-melanogenic, and anticancer properties in various cell types [14,15].

However, gallic acid's low solubility, limited bioavailability, and susceptibility to instability limit its usefulness in the pharmaceutical industry. In order to enhance the efficacy of targeted drug delivery and the solubility and bioavailability of GA by reducing the particle size, it was formulated in nanoparticle form [12].

In this study, GA was chosen as both the reducing agent and the coating material to create zinc-gallic acid nanoparticles (Zn-GANPs). These newly synthesized nanoparticles were subsequently assessed *in vivo* in a rat model with HCC. We used flow cytometry (FACS) and ELISA to detect transforming growth factor-Beta 1 (TGF- β 1), cell cycle, alpha-fetoprotein (AFP), liver caspase-3, and B-cell lymphoma 2 (Bcl-2). These are all proteins that play a part in the growth, progression, and apoptotic cell death. Moreover, reactive oxygen species (ROS) levels mediated lipid peroxidation, thiobarbituric acid reactive substances (TBARS), malondialdehyde (MDA), which induced nuclear factor kappa-light-chain-enhancer of activated B cells transcription factor (NF- κ B p65) led to inflammatory responses. Furthermore, glutathione (GSH), along with the activity of catalase (CAT), alanine transaminase or alanine aminotransferase (ALT), aspartate transaminase or aspartate aminotransferase (AST), and gamma-glutamyl transferase (GGT or γ -GT) activities, as well as the concentrations of albumin, globulin, total protein, and total bilirubin were determined.

2. Materials and methods

2.1. Materials

DEN, Folin-Ciocalteu reagent, polyvinyl alcohol (PVA), zinc nitrate and GA standards and silica gel were obtained from Sigma Aldrich (St Louis, MO, USA).

2.1.1. Experimental animals

Study rodents were 40 male Wistar rats measuring 120–150 g. A 12/12-h light/dark cycle was maintained in a temperature- and light-controlled chamber for rats. The animals lived in wire-bottomed stainless-steel cages with free food and water. The experiments were conducted following the guidelines established by the Research Ethics Committee of October 6 University, Egypt, with Registration No. PRE-Ph-2304007. The present study adhered to the principles outlined in [16].

2.1.2. Plant material

Dried, powdered peels from pomegranate fruits were gotten from an Egyptian local market.

2.2. Methods

2.2.1. Extraction and fractionation of *Punica granatum* L. peels

Five hundred grams of powdered peels underwent thorough extraction, with 80% methanol being used for one batch, and another 500 g being extracted using distilled water. These extraction procedures resulted in dense extracts of 60 g and 70 g, respectively. The aforementioned sample (80% methanol extract) was then mixed in 100 ml of distilled water and subjected to subsequent extractions with n-hexane and ethyl acetate in a separatory funnel. Both solvents were evaporated using a rotary evaporator under reduced pressure (Buchi R-210 evaporator, Flawil, Switzerland), resulting in the production of hexane (4 g) and ethyl acetate (21 g) fractions.

2.2.2. Total polyphenol content (TPC)

The TPC of the prepared extracts and fractions was quantified utilizing the Folin-Ciocalteu colorimetric method, following the procedure outlined in a previously described method of [17].

2.2.3. Isolation of gallic acid (GA)

The ethyl acetate fraction from methanol extract was chromatographed on a silica gel 60–120 CC (6 cm \times 85 cm, 260 g). The column was developed with a solvent gradient of chloroform:methanol, starting with 100:0 and gradually transitioning to 0:100 in half-unit increments, and fractions (50 ml each) were collected. Tracking of gallic acid content in different fractions was carried out by comparing the spots with authentic gallic acid through UV detection at 254 nm using TLC. Notably, dark spots were observed, displaying good separation with an R_f value of 0.4 when using a mobile phase comprising toluene: ethyl acetate: formic acid in a ratio of 3.5:6:0.5. In a different solvent system, chloroform: ethyl acetate: acetic acid (4.5:5:0.5), a dark spot appeared with an R_f value of 0.36.

With gradient elution using chloroform: methanol mixture. Subsequently, the polarity was increased in steps to achieve ratios of 9:1, 8.5:1.5, and 8:2, gradually transitioning to pure methanol.

2.2.4. Biosynthesis of Zn-GANPs

2.2.4.1. ZnO nanoparticles synthesis by gamma-irradiation. The aqueous solution of polyvinyl alcohol (PVA) with a weight percentage of 4% and a molecular weight of 89,000 (Sigma-Aldrich) was supplemented with a stock solution of zinc nitrate (Zn (NO₃)₂, Sigma-Aldrich) at a concentration of 0.2 mmol/L. The solution was then agitated for a duration of

1 hour at a temperature of 70 °C, followed by the introduction of nitrogen gas into the solution for a period of 30 minutes. The final solution was subjected to irradiation doses of 50 kGy utilizing a Co-60 γ -ray source chamber with a dose rate of 0.83 kGy/h, as conducted by the NCRRT, EAEA. To get a refined ZnO nanopowder (2.5 mmol/L), the irradiation sample underwent a washing process using centrifugation with deionized water and ethanol. Subsequently, the sample was subjected to a drying period of 10 hours at a temperature of 90 °C under air pressure.

2.2.4.2. Biosynthesis of Zn-GANPs. Subsequently, a volume of 2.0 ml of a 10 mM solution of GA was introduced, followed by pH adjustment to 11.0 using a 1.0 M solution of NaOH. The reaction was maintained at RT for a duration of 30 minutes. The nanoparticles underwent a process of condensation and purification using centrifugation at a speed of 15000 rpm for a duration of 10 minutes, followed by three subsequent washes using double-distilled water.

2.2.5. Characterization of Zn-GANPs

2.2.5.1. Ultraviolet- visible (UV-Vis) analysis. JASCO twin beam spectrophotometer V-570 UV/VIS/NIR analyzed Zn-GANPs' UV/Vis spectra from 190 to 900 nm to determine particle size and distribution.

2.2.5.2. Transmission electron microscopy TEM analysis. TEM evaluated the size, type, and form of synthesized Zn-GANPs. Sonication of the nanoparticle solution for 5 minutes improved particle dispersion and prevented copper grid agglomeration. After that, TEM samples of Zn-GANPs were generated by dropping nanoparticle solutions on carbon-coated copper grids and letting water evaporate. Nanoparticle form and size were assessed using TEM micrographs. A high-resolution transmission electron microscope (HR-TEM; JEOL, JEM2100, Electron Microscope, Japan) assessed solution morphology and particle size.

2.2.5.3. Size-distribution analysis (DLS). Dynamic light scattering examined Zn-GANP size distribution. At 25°C and 90°C scattering angle, photon correlation spectroscopy (PCS) assessed particle sizes.

2.2.5.4. Fourier-transform infrared (FTIR) spectroscopy. The resulting sample was analyzed utilizing the KBr disc technique on a Nexus 670 FTIR (USA) spectrometer in the 400–4000 cm^{-1} range.

2.2.6. Experimental design

Forty adult male Wistar rats were (180 \pm 20 g) allocated randomly into four equal groups (10 rats/group) of similar size. The groups were distributed as follows: Group I (Normal untreated control group), rats received normal saline. Group II (liver carcinogenesis DEN group) rats being orally administered with DEN (20 mg/kg b.wt.) 5 times per week for a duration of 8 weeks. Group III (Zn-GANPs) rat for 5 weeks, were injected intraperitoneally by Zn-GANPs (20 mg/kg b.wt) [18]. Group IV (DEN + Zn-GANPs treated group), rats got DEN like group II and subsequently treated with Zn-GANPs like group III until the 13-week trial was ended [19]. Finally, we collected blood samples and liver tissues from animals.

2.2.7. Assessment of serum hepatic functions

The ALT and AST activities were calculated using [20]. We measured serum GGT or γ -GT activity in accordance with [21]. The concentrations of albumin, globulin, and serum total protein were ascertained in accordance with [22]. The total bilirubin level was detected according with [23].

2.2.8. Determination of liver antioxidant

Liver catalase activity was measured using [24]. We evaluated GSH in liver tissue using [25] assay. TBARS was used to assess liver tissue

MDA concentration using [26] technique.

2.2.9. Assay of AFP, caspase –3, Bcl-2 and NF κ B p65

The ELISA Kit (Biomatik, Ontario, Canada) was used to detect serum AFP, as well as liver caspase-3, Bcl-2, and NF κ B p65, following the guidelines provided by the manufacturer.

2.2.10. Flow cytometric analysis to TGF- β 1 and cell cycle in liver tissue

The fresh tissue specimens were prepared in accordance with the methodology outlined in reference [27]. The FACS caliber flow cytometer, manufactured by Becton Dickinson in Sunnyvale, CA, USA, was employed at Mansoura Children Hospital to assess the levels of (TGF- β 1) and determine the distribution of cells across various phases of the cell cycle (G0/1, S-phase, G2/M) for both diploid and aneuploid cycles. Additionally, parameters such as coefficient of variation (CV), percentage of apoptotic cells (Apoptosis%), DNA index (DI), diploid percentage, and aneuploidy percentage were also evaluated [28].

2.2.11. Histopathological studies

Liver tissues were fixed in 10% formalin/saline for 24 hours. Serial dilutions of alcohol (70% methanol, 95% ethanol, and 100% ethanol) were employed to dehydrate samples after tap water washing. After clearing in xylene, specimens were embedded in paraffin at 56°C in a hot air oven for 24 hours. Slidge microtomes sectioned paraffin wax tissue blocks at 4 microns. On glass slides, tissue slices were deparaffinized and stained with H&E stains according to [29].

2.2.12. Statistical analyses

All statistical studies utilized SPSS 22 and GraphPad Prism 8. Results were analyzed by a one-way analysis of variance and mean comparison significance $P \leq 0.05$ in GraphPad. Duncan's test was used to determine inter-group homogeneity by comparing groups many times.[30].

3. Results

3.1. Assessment of total phenolic content (TPC) concentration

The TPC finding were quantified in milligrams of Gallic Acid Equivalent (mg GAE/g) per gram of plant dry weight. The highest TPC was recorded in the ethyl acetate fraction of the methanol extract from pomegranate peels, amounting to 95.52 \pm 0.80 mg GAE/g. It was closely followed by the methanol extract from pomegranate peels at 83.66 \pm 0.67 mg GAE/g. In contrast, the aqueous extract of pomegranate peels displayed a TPC of 49.55 \pm 0.87 mg GAE/g. Notably, the ethyl acetate fraction of the aqueous extract from pomegranate peels exhibited the lowest TPC at 27.80 \pm 1.1 mg GAE/g.

3.2. Characterization of the isolated compound from pomegranate peel

The isolated compound from pomegranate peel was pale-yellow in color with Rf 0.26 in mobile phase hexane: ethyl acetate: acetic acid, (2:1:0.3). The following peak data from the compound's ^1H and ^{13}C NMR spectra were used to confirm its chemical structure: ^1H NMR (400 MHz, CD $_3$ OD- d_6): δ 9.1207 (1 H, H-7, s) 7.0952 (2 H, H-2 & H-6, s) 4.9700 (1 H, H-3, H-4, H-5, s). ^{13}C NMR (100 MHz, CD $_3$ OD): δ 120.55 (C-1), 109.00 (C-2 & C-6), 144.98 (C-3 & C-5), 138.23 (C-4) and 169.11 (C-7). The melting point of the isolated compound was determined to be within the range of 248–250 °C. Furthermore, the thin-layer chromatography characteristics and the melting point of the compound were consistent with those of authentic gallic acid, confirming their similarity. From all the presented evidence, the substance isolated from pomegranate peel was conclusively identified as gallic acid (1.5 g).

3.3. Biologically synthesized Zn-GANPs nanoparticles were characterized by

3.3.1. Zn-GANPs UV-visible spectroscopy

The UV-vis spectra of Zn-GANPs showed two peaks of characteristic absorption band at 215 nm and 263 nm, it is also important that these spectra are almost the same as the UV spectrum of free GA. The absorption spectrum of (GA) exhibits two peaks in the UV range. One at 225 nm and the other at 260 nm. The shift in band to Zn⁺⁺ ion.

The UV-vis spectra of Zn-GANPs showed two peaks one of characteristic absorption band at 263 nm, Fig. 1 A.

3.3.2. Zn-GANPs TEM

TEM photos were investigated the surface morphology, size and shape in Zn-GANPs. The observed morphology of Zn-GANPs showed almost spherical shape with size 38.8 nm, Fig. 1B. Physical characterization of NPs is commonly characterized using transmission electron microscope (TEM). TEM confirmed that the Zn-GANPs were nearly spherical in shape, with good size 38.8 nm.

3.3.3. Zn-GANPs DLS

Nanoparticles size distribution was estimated using DLS technique in aqueous media for Zn-GANPs. As shown in the Fig. 2, Zn-GANPs exhibited size distribution with mean hydrodynamic radius of about 20–100 nm. The main peaks with an average size of 28.2, 24.36, 32.67 and 21.04 nm contained 25.5, 24.7, 17.4 and 13.2%, respectively of the nanoparticles and 0.292 poly dispersity index (PDI).

3.3.4. Zn-GANPs FT-IR

The FT-IR spectra of Zn-GANPs, as seen in Fig. 3, exhibits two distinct bands at 3784 and 3720 cm, which may be ascribed to the stretching of

free phenolic O–H bonds. Additionally, another band at 3187 cm is observed, which is associated with the stretching of acidic O–H bonds. The observed peak at 1552 cm⁻¹ maybe due to C=C bond stretching vibration inside the aromatic ring. The band seen at a wavenumber of 1351 cm is a result of the bending vibration of the –CH– group within the benzene ring. Similarly, the 1035 cm band is the C–O bond stretching vibration within the carboxylic group. Additionally, the band observed at 746 cm may be linked to the δ CC vibrations inside the benzene ring.

The FT-IR spectrum of the sample Zn-GANPs showed FTIR peaks representing functional groups found in the Gallic acid. That mean the nanoparticles formation did not involve chemical reactions but physical interaction keeping active functional groups which participate in nanoparticles activity.

3.3.5. Effect of Zn-GANPs on liver functions in different groups

Fig. 4 demonstrates an elevation in AST, ALT, GGT activities significantly, and total bilirubin level, by 51%, 111.2%, 119%, and 95.4%, respectively, in the liver cancer group caused by DEN in comparison to the control group. The I.P delivery of Zn-GANPs to normal rats did not result in a statistically significant alteration in AST, ALT, GGT activities, and the level of total bilirubin, as compared to the control group.

The administration of Zn-GANPs in the group with liver cancer group produced by DEN resulted in a statistically insignificant reduction in total bilirubin, AST, ALT, and GGT levels. The observed percentage changes were 22.1%, 13.8%, 57%, and 50%, respectively, in comparison to the control group.

3.3.6. Zn-GANPs affect serum proteins

Serum total protein, albumin, globulin, and A/G ratio in normal and treated animals are shown in Table 1. DEN-induced liver cancer rats had lower serum total protein, albumin, and A/G ratios (–25%, –60%, and 9.2%, respectively) than normal rats. Compared to normal control rats, DEN-induced liver cancer animals had a non-significant globulin decrease (–50%). Compared to the normal control group, Zn-GANPs i.p. administration to normal rats did not modify serum total protein, albumin, globulin, or A/G. Serum total protein increased non-significantly (–13.3%) in rats with liver cancer and a significant increase in albumin, globulin, and A/G levels (–35.9%, 26.8%, and –49%, respectively) post Zn-GANPs treatment as compared to the normal control group.

3.3.7. Effect of Zn-GANPs on serum AFP, liver tissue NF- κ B P65, Bcl2 and caspase-3 levels in normal and DEN-induced liver cancer

Fig. 5 depicts the caspase-3, AFP, liver NF- κ B P65 and Bcl₂ levels in the in normal and treated animals. Results showed a significant increase in serum AFP, liver NF- κ B P65 and Bcl₂ levels (0.42±0.1, 179.1±6.25, and 119.1±2.7, respectively) and a significant decrease in liver caspase-3 level (1.14±0.17) in DEN induced liver cancer rats as compared to normal control rats.

Administration of Zn-GANPs i.p to normal rats showed non-significant changes in serum AFP, liver tissue NF- κ B P65, Bcl₂, and caspase-3 concentrations when compared to normal control group. Treatment with Zn-GANPs resulted in a non-significant decrease in serum AFP level (0.33±0.04), significant decrease in liver NF- κ B P65 and Bcl₂ levels (106.1±4.65, 70.35±3.15, respectively) and a significant increase in liver caspase-3 level (4.35±0.55) when compared with DEN group.

3.3.8. Effect of Zn-GANPs on liver tissue catalase activity, GSH, and L-MDA levels in normal and DEN-induced liver cancer

To assess liver oxidative damage in DEN-exposed rats, catalase activity, GSH, and L-MDA levels were evaluated (Fig. 6).

Fig. 6 shows that DEN-induced liver cancer in rats decreased liver Catalase activity and GSH concentration (–44.5% and –53.5%, respectively) and increased L-MDA concentration (124.5%) compared to normal control rats. Normal rats given Zn-GANPs i.p. had no significant

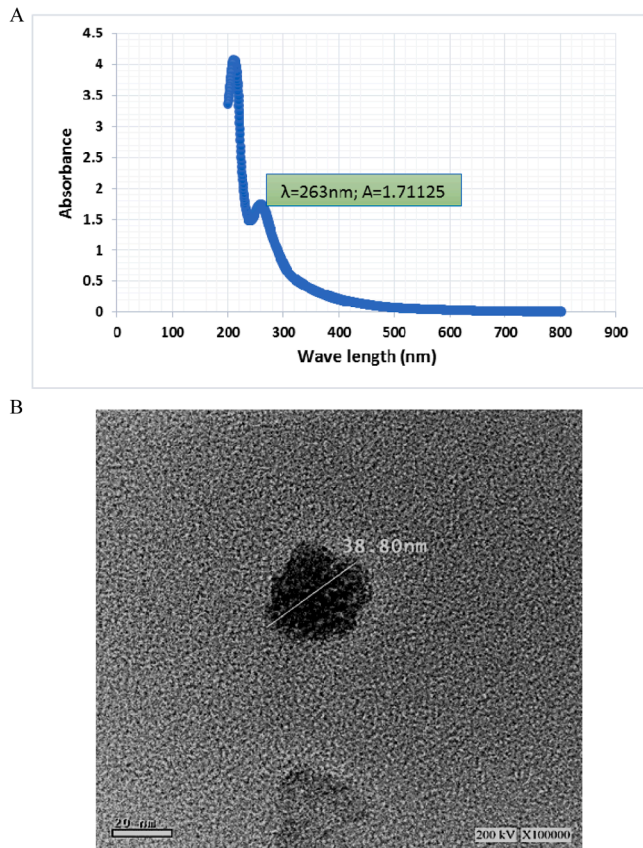


Fig. 1. (A) UV-Vis spectra of Zn-GANPs aqueous solution. (B) TEM image of Zn-GANPs.

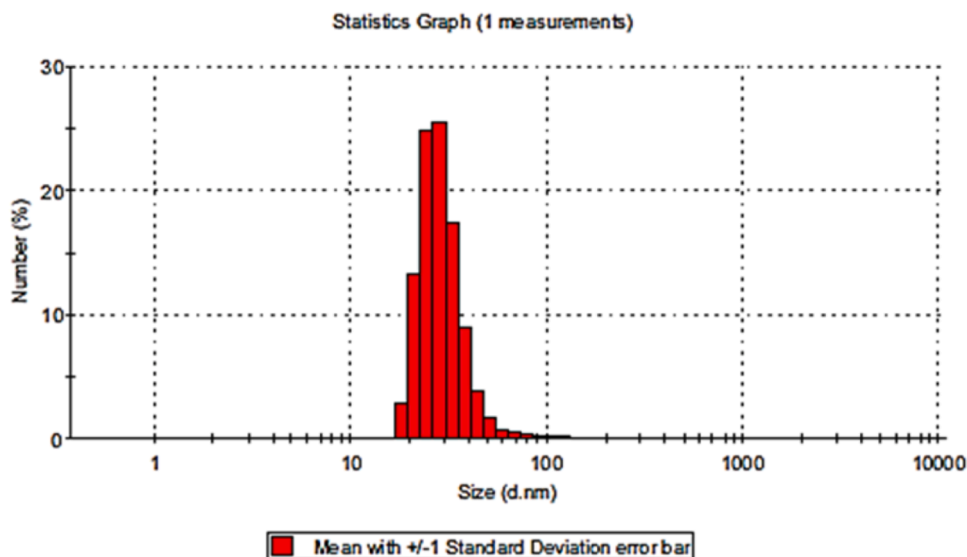


Fig. 2. DLS intensity-based size distribution histograms of Zn-GANPs.

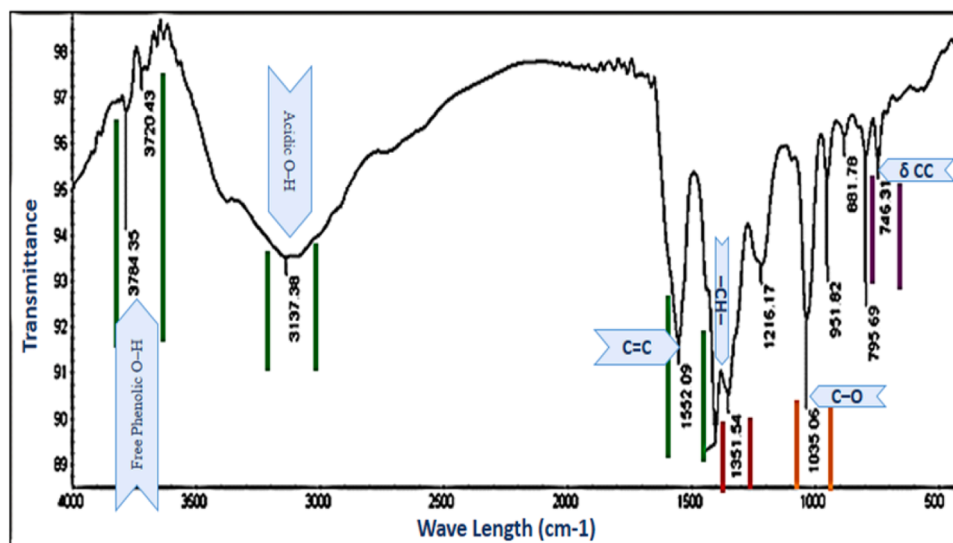


Fig. 3. Fourier transform infrared spectra for Zn-GANPs.

change in liver tissue catalase activity, GSH, or L-MDA levels. Zn-GANPs did significantly modify liver catalase activity, GSH, or L-MDA concentrations compared to DEN group (55.7%, 65.0%, and -34.9%, respectively).

3.3.9. Effect of Zn-GANPs on TGF- β 1% in liver tissue in different groups

Effect of Zn-GANPs on TGF- β 1% of DEN- induced hepatocellular carcinoma in male rats is presented in (Fig. 7). Significant TGF- β 1% rise was reported in DEN-induced hepatocellular cancer group compared to control group (91.61% change). Treatment with Zn-GANPs showed a significant decrease in TGF- β 1% when compared with HCC group by 29.1% of change. A non-significant increase in TGF- β 1% in Zn-GANPs group when compared with control group by 10.68% of change.

3.3.10. Effect of Zn-GANPs on sub G0%, S phase G2M% and G1 apoptosis in liver tissue of different groups

Effect of Zn-GANPs sub G0%, S phase G2M% and G1 apoptosis in liver tissue DEN- induced hepatocellular carcinoma in male rats is graphically illustrated in (Fig. 9). As shown in Fig. 8, the number of cells in G0/G1 significantly decreased, S phase increased and G2/M increased

in Zn-GANPs + DEN treated group ($p < 0.05$) ($53.84 \pm 4.1\%$, $27.5 \pm 2.17\%$, and $20.1 \pm 3.2\%$, respectively) compared to DEN group ($86.9 \pm 3.47\%$, $1.1 \pm 0.15\%$, and $3.3 \pm 0.47\%$, respectively).

3.3.11. Effect of Zn-GANPs on histopathological alterations in liver tissue of different groups

The liver of control and Zn-GANPs animals showed normal histological structure that is characterized by normal central vein and surrounding hepatocytes in the parenchyma (Fig. 9 A,B). Liver of rats received DEN showed that strands of fibrous tissue dividing the vascular degenerated and coagulative necrosis hepatocytes in the parenchyma into lobules. (Fig. 9 C,D). These findings proved the credibility of the applied experimental carcinogenesis model. Liver of treated animals (DEN+ Zn-GANPs) showed improvement characterized by that hepatocytes all over the parenchyma showed diffuse vacuolar degenerations as well as fatty change associated with very fine strands of fibroblastic cells proliferation in between (Fig. 9 E,F,G).

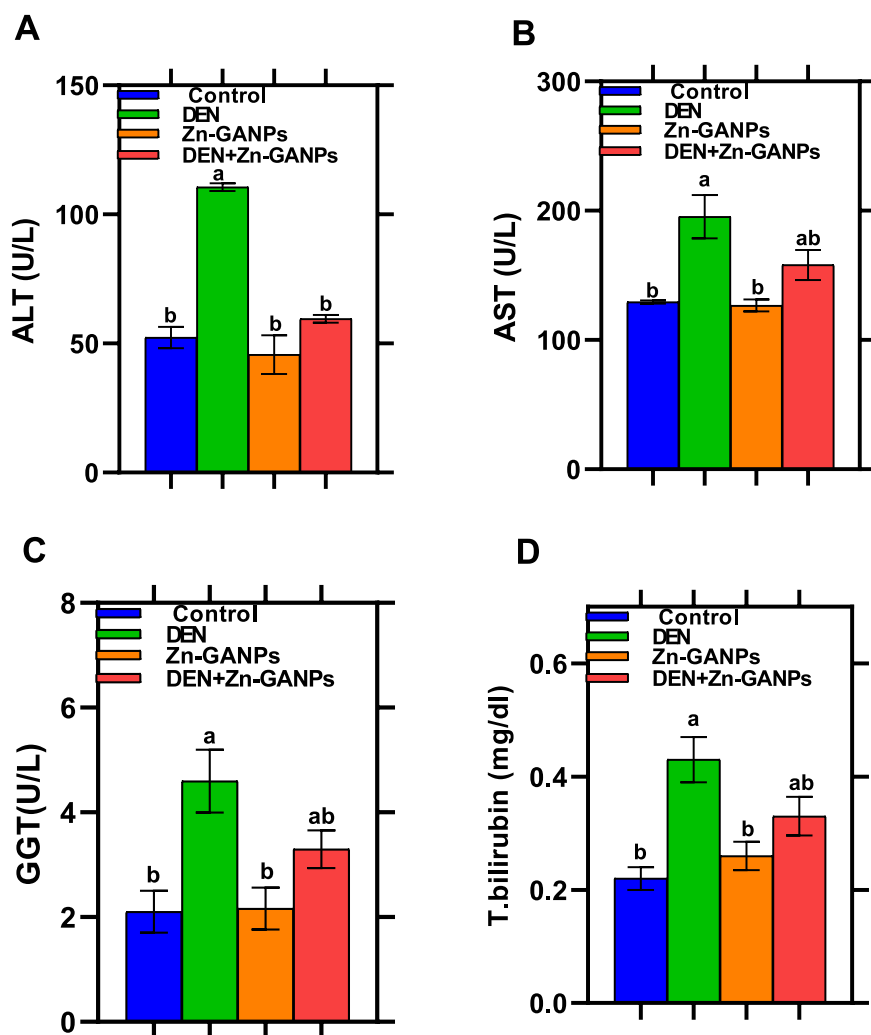


Fig. 4. Effect of Zn-GANPs on serum A- ALT. B- AST. C- GGT. D- Total bilirubin, in hepatocarcinogenesis induced in rats. Data are expressed as the mean \pm SD (n = 10). Columns carrying different letters are significantly different (one-way ANOVA) ($p < 0.05$).

Table 1

Zn-GANPs' impact on the levels of albumin, globulin, total protein, and the A/G ratio.

Parameters Groups	Total protein (mg/dl)	% of change	Albumin (mg/dl) Alb	% of change	Globulin (mg/dl)	% of change	A/G ratio	% of change
Control	6.0 \pm 0.17 ^b		3.23 \pm 0.24 ^b		2.5 \pm 0.2 ^b		1.29 \pm 0.06 ^b	
DEN	4.5 \pm 0.2 ^a	-25	1.77 \pm 0.2 ^a	-60.7	2.73 \pm 0.03 ^a	9.2	0.64 \pm 0.08 ^a	-50
Zn-GANPs	5.8 \pm 0.26 ^b	-3.3	3.1 \pm 0.2 ^b	-4	2.66 \pm 0.06 ^{ab}	6.4	1.17 \pm 0.05 ^b	-9
DEN+Zn-GANPs	5.2 \pm 0.22 ^{ab}	-13.3	2.07 \pm 0.14 ^a	-35.9	3.17 \pm 0.08 ^a	26.8	0.65 \pm 0.03 ^a	-49

4. Discussion

Hepatocyte loss and compensatory proliferation are prevalent in chronic inflammation-related HCC. DEN, a well-studied substance, causes HCC in animals. DEN promotes DNA damage, reactive oxygen species accumulation, and hepatocyte death via the JNK pathway in the DEN-induced HCC model [31]. Since liver is the major site of DEN metabolism, ROS including hydroxyl, superoxide, alkoxyl, and peroxy radicals, singlet oxygen, ozone, anions, and hydrogen peroxide cause cancer [32,33]. Cytochrome P-450 (CYP2E1) converts DEN to its dynamic ethyl radical metabolite, which interacts with DNA to cause mutations and cancer [34]. In this study, Zn-GANPs were tested *in vivo* against HCC in male rats. The nanoparticles displayed minimal toxicity and adverse effects up to 500 mg/kg. DEN, a major environmental carcinogen, may promote ROS production, oxidative stress, and cellular

damage [35]. Metal ions like Zn is essential for life. Other than being a co-factor of Superoxide dismutase SOD1 and SOD3, Zn maintains protein sulphhydryl groups, protects against vitamin E depletion, stabilizes membrane structure, and maintains tissue metallothionein concentrations, powerful free radical scavengers. Thus, Zn supplementation may boost antioxidant defenses [15].

Plasma membrane-associated NADPH oxidases, produce $\cdot\text{O}^{-2}$ from oxygen utilizing NADPH as an electron source. Zinc, an effective antioxidant reduces ROS by inhibiting NADPH oxidase. Zinc competes with Fe and Cu ions for binding to cell membranes and proteins, therefore displaces these redox active metals that produce $\cdot\text{OH}$ from H_2O_2 . Zinc protects biomolecules from oxidation by binding to (SH) sulphhydryl groups. Also, Zinc has been shown to enhance the levels of antioxidant proteins, chemicals, and enzymes such as GSH, catalase, and SOD, while simultaneously reducing the expression of Inducible nitric oxide

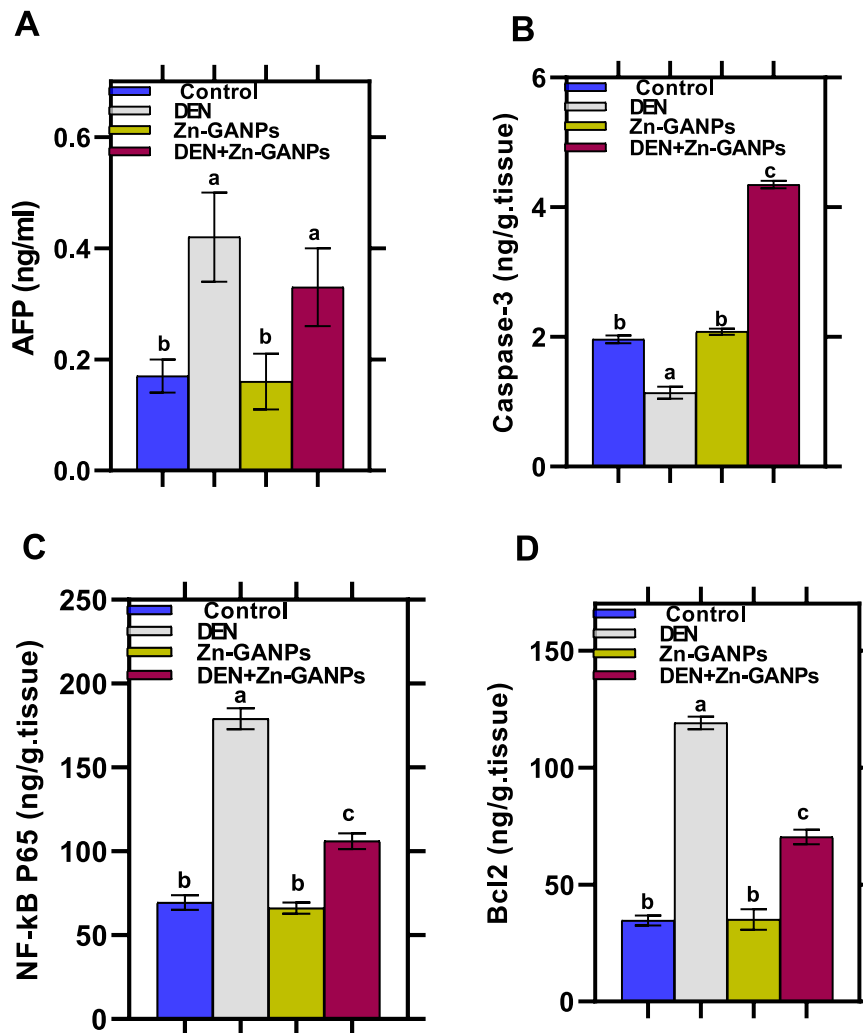


Fig. 5. Effect of Zn-GANPs on A- AFP. B- Caspase-3. C- NF-κB p65. D- Bcl2. in hepatocarcinogenesis induced in rats. Data are expressed as the mean \pm SD (n = 10). Columns carrying different letters are significantly different (one-way ANOVA) ($p < 0.05$).

synthase (iNOS), NADPH oxidase, and lipid peroxidation. Further, zinc promotes the production of metallothionein (MT), a cysteine-rich protein that effectively scavenges $\cdot\text{OH}$ ions [36].

The GA molecule has antioxidant properties and may protect biological systems against ROS including hydroxyl ($\text{HO}\cdot$), superoxide ($\text{O}_2^{\cdot-}$), and peroxy ($\text{ROO}\cdot$), as well as non-radicals such hydrogen peroxide (H_2O_2) and hypochlorous acid (HOCl). In addition, some plant extracts have shown effective antiradical and anticancer effects, and GA is the main antioxidant component responsible for this [37].

4.1. Effect of Zn-GANPs on liver functions in normal and DEN-induced liver cancer

DEN treatment to male rats increases serum AST and ALT, indicating hepatocellular injury [38]. After plasma membrane rupture and oxidative stress-induced cellular damage, [39]. cytoplasmic AST and ALT are released into the circulation following cellular injury making them the most sensitive indicators of liver impairment [40]. Overproduction of enzymes in tumor cells may have increased cell membrane permeability, releasing enzymes into serum [35]. Similarly, the elevated γ -GT in rat sera may be due to the enzyme's release from the plasma membrane, suggesting cell membrane damage [41], highlighting its anti-oxidative stress function. The harmful effects of Few studies have examined the impact of Zn-GANPs on HCC models, however we found GA and Zn effects on enzyme activity. Zn-GANPs dramatically lowered marker

enzyme activity in DEN-treated rats. This suggests that Zn-GANPs protect the liver by preserving plasma membrane integrity and preventing hepatic enzyme leakage. This may explain why Zn-GANPs restore liver enzyme activity. Gallic acid is a good free radical scavenger and tumor cell line differentiation and death inducer [42]. GA considerably decreased ALT and AST [43].

The male rats with HCC showed higher blood total bilirubin than normal rats. Toxic or ischemic liver damage raises serum conjugated bilirubin. Acute viral hepatitis hyperbilirubinemia is proportional to hepatocyte histological damage and illness duration [44].

In addition, HCC and non-HCC groups had significantly different blood total bilirubin levels. HCC patients with abnormal bilirubin had a poorer outcome. These studies link bilirubin to HCC aggressiveness [45]. Further it was also reported that DEN treatment raised blood total bilirubin in HCC-induced albino mice. Mass blockage of the conjugation process and increased release of unconjugated bilirubin from injured hepatocytes [46]. Additionally, carcinogen's toxic action on hepatocytes and sinusoidal cells may cause the central vein's reticulin network to collapse, causing bleeding and bilirubin production [47].

In this research, Zn-GANPs significantly reduced blood total bilirubin compared to DEN, perhaps owing to Gallic acid and Zn's antioxidant qualities that counteracted DEN's harmful effects. Gallic acid and zinc stabilize cell membranes and protect the liver from ROS-mediated liver damage, which may explain Zn-GANPs' impact on blood bilirubin [48].

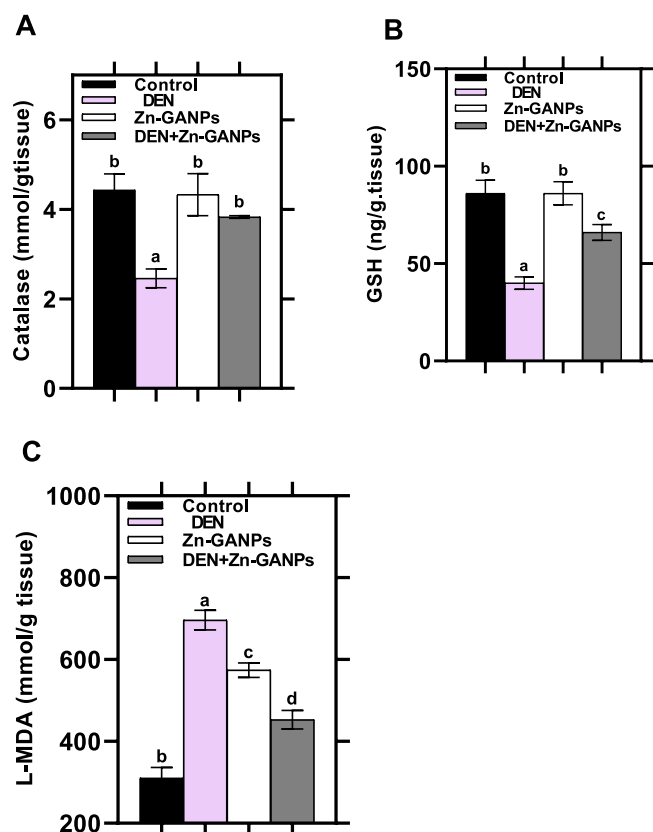


Fig. 6. Effect of Zn-GANPs on liver tissue A- catalase activity. B- GSH. C- L-MDA. Data are expressed as the mean \pm SD (n = 10). Columns carrying different letters are significantly different (one-way ANOVA) (p < 0.05).

4.2. Zn-GANPs affects serum proteins in normal and liver cancer

DEN-induced HCC showed a substantial reduction in serum total protein, albumin, and A/G, but globulin levels increased non-significantly compared to normal rats. Serum total protein assists in transport, immunological defense, blood coagulation, and inflammatory defense [49]. The liver synthesizes albumin, which transfers vital fatty acids from adipose to muscular tissue. Therefore, low albumin levels may indicate liver illness [50]. Albumin/Globulin (A/G) ratio is the computed ratio of these serum proteins. Low A/G is reported in liver, renal, myeloma, inflammatory, and other illnesses [50]. A Low blood albumin has consistently been linked to a high risk of HCC [51].

HCC is linked to decreased serum total protein [52]. DEN-induced HCC frequently causes reduced albumin and total protein serum levels, indicating liver dysfunction and infection [23]. Cross et al., [53] ascribed hypoalbuminemia to enhanced catabolism rather than synthesis impairment owing to carcinogen's toxic impact, which increases ROS generation. Free radicals damage proteins that affect cell activity, membrane structure, and function. Hypoalbuminemia may also develop from liver diseases that reduce albumin production [54].

In this work, Zn-GANPs increased serum total protein and albumin concentrations in HCC-induced rats compared to DEN. Zn-GANPs may be inhibited by drugs that scavenge ROS, limit their production, or boost zinc's antioxidant capacity [55]. Gallic acid is also expected to be a top peroxy radical scavenger in nonpolar (lipid) environments. Scavenges hydroxyl and hydroperoxyl radicals at diffusion-limited and rate constant rates, respectively. Gallic acid is a flexible scavenger that can quickly deactivate several ROS and RNS via electron transfer at physiological pH [56].

4.3. Zn-GANPs affects AFP, liver tissue NF- κ B P65, Bcl2 and caspase-3 levels in normal and DEN-induced liver cancer

In this research, rats given DEN had significantly higher AFP in the HCC group than the control group [23]. In hepatocellular carcinoma, AFP levels are increased [57]. Hepatotoxic substances, or hepatocarcinogens, DEN have the potential to increase AFP levels associated with HCC. AFP's high specificity of over 90% for determining hepatocarcinoma patients prognosis [58]. Zn-GANP therapy decreased AFP in this research, suggesting anti-inflammatory and anticancer capabilities contributed to the beneficial outcome. Zinc supplementation reduced plasma oxidative stress indicators and inflammatory cytokines in older adults [59].

The findings showed that DEN-induced liver cancer in rats had a much lower liver caspase-3 content than the control group. Caspase-3 deficiency markedly exacerbated DEN-induced HCC development, hepatocyte apoptosis, and compensatory proliferation. Caspase-3 deficiency also boosted p38 mitogen-activated protein kinase (p38 MAPK) activity. Deleting caspase-3 led to enhanced p38 activation by Interleukin-1 alpha (IL1 α) and Tumor Necrosis Factor Alpha (TNF α) in primary mouse hepatocytes. In caspase-3-deficient animals, p38 inhibition prevented DEN-induced hepatocyte apoptosis, compensatory proliferation, and HCCs. We found that caspase-3 suppresses p38 activation and hepatocarcinoma cell death to prevent chemical-induced hepatocarcinogenesis [31].

In rats with DEN-induced liver cancer, Zn-GANP therapy increased caspase-3 levels significantly compared to the control group. Two majors, connected apoptotic processes are death receptor (extrinsic) and mitochondrial-mediated (intrinsic). Proenzymes of the caspase family mediate apoptosis. After activation, caspases inactivate anti-apoptotic proteins, halt DNA replication, and reorganize the cytoskeleton to kill cells. Upstream regulators like caspase-8 and -9 regulate caspase-3, which is important for apoptosis. caspase-8 and -9 regulate intrinsic and extrinsic apoptosis. GA activates caspase-3 to promote cell death [60].

The study found a substantial rise in NF- κ B levels in rats with DEN-induced liver cancer in comparison to the control group. NF- κ B is the main orchestrator of the inflammation-fibrosis-cancer axis. NF- κ B has several roles in hepatocytes, immune cells, and fibrogenic cells, creating an optimal milieu for HCC [61]. Nuclear factor-kappa B is inappropriately activated in certain human hepatocellular carcinomas. The expression of NF- κ B family proteins was higher in hepatocellular carcinomas compared to neighboring non-neoplastic liver tissue [62]. Wan et al. [63] found that DEN-induced HCC in rats dramatically raised NF- κ B p65 concentrations.

Zn-GANP therapy lowered NF- κ B levels, reducing liver fibrosis and necrotic inflammation. A strong association was detected between liver NF- κ B levels and lipid peroxidation, indicating that oxidative stress plays a significant role in hepatic inflammation and fibrosis in the DEN group. Gallic acid's antioxidant activities provide anti-inflammatory and anti-fibrotic benefits, reducing NF- κ B concentration in ulcerative colitis [43,64]. Zinc reduces NF- κ B activation and inflammatory cytokine production (TNF- α , IL-1 β , and IL-8) via deregulation of NF- κ B activity [65].

In rats with DEN-induced liver cancer, Bcl-2 concentration was significantly elevated in comparison to control. Functionally, Bcl-2 family members are anti- or pro-apoptotic. The balance between these two groups may affect tumor cell fate. This balance favors anti-apoptotic tumor cells in HCC, resulting in cell death resistance and fast multiplication. The BCL-2 family of proteins controls the intrinsic apoptotic pathway in response to cellular stressors such as DNA damage, γ -irradiation, oncogene activation, and growth factor withdrawal [66]. DEN treatment increased Bcl-2 expression as a transcription target [23].

The current study found that Zn-GANP therapy significantly decreased Bcl-2 activity in rats that had been treated with DEN compared to the rats that had not been treated. The antioxidant, anti-

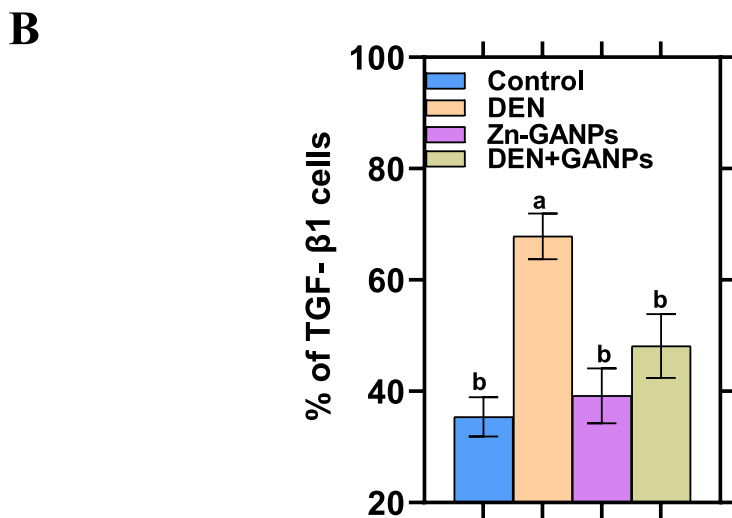
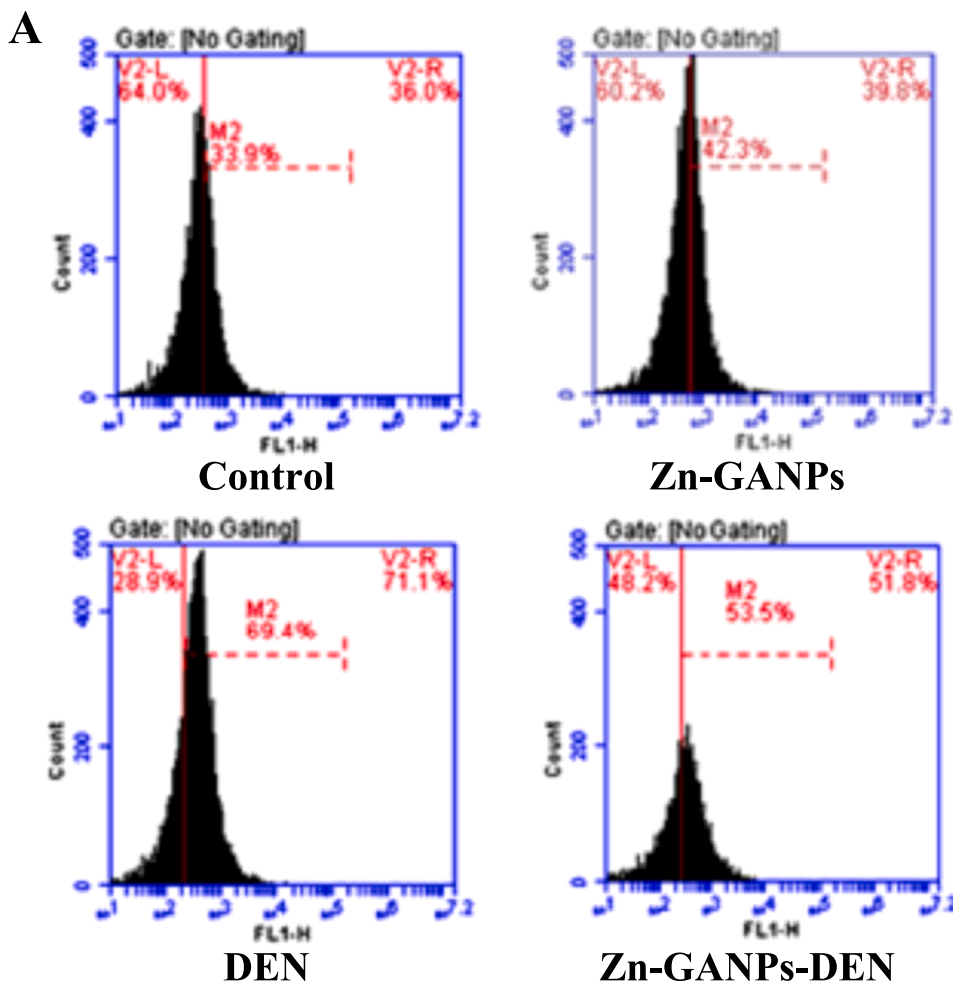


Fig. 7. Effect of Zn-GANPs on TGF-β1% of DEN- induced hepatocellular carcinoma of different groups. (A) Flow cytometry of TGF-β1%. (B) Histogram of TGF-β1%. Each experiment was repeated three times, data are expressed as the mean ± SD (n = 10). Columns carrying different letters are significantly different (one-way ANOVA) (p < 0.05).

inflammatory, and DNA-damaging properties of Zn-GANPs may suppress cell apoptosis. In cell lines, gallic acid caused JNK phosphorylation and Bcl-2 downregulation [67]. Zinc sulphate raised intracellular zinc levels in prostate cancer cells, causing apoptosis. Increased zinc concentration may cause apoptosis by increasing zinc transporter expression and decreasing Bcl-2 [68].

4.4. Effect of Zn-GANPs on liver tissue catalase activity, GSH, and L-MDA levels in normal and DEN-induced liver cancer

Tissue catalase activity and GSH levels were significantly declined in HCC in comparison to controls. DEN increases biological free radicals and oxidative stress [69]. Enzymatic antioxidants like glutathione

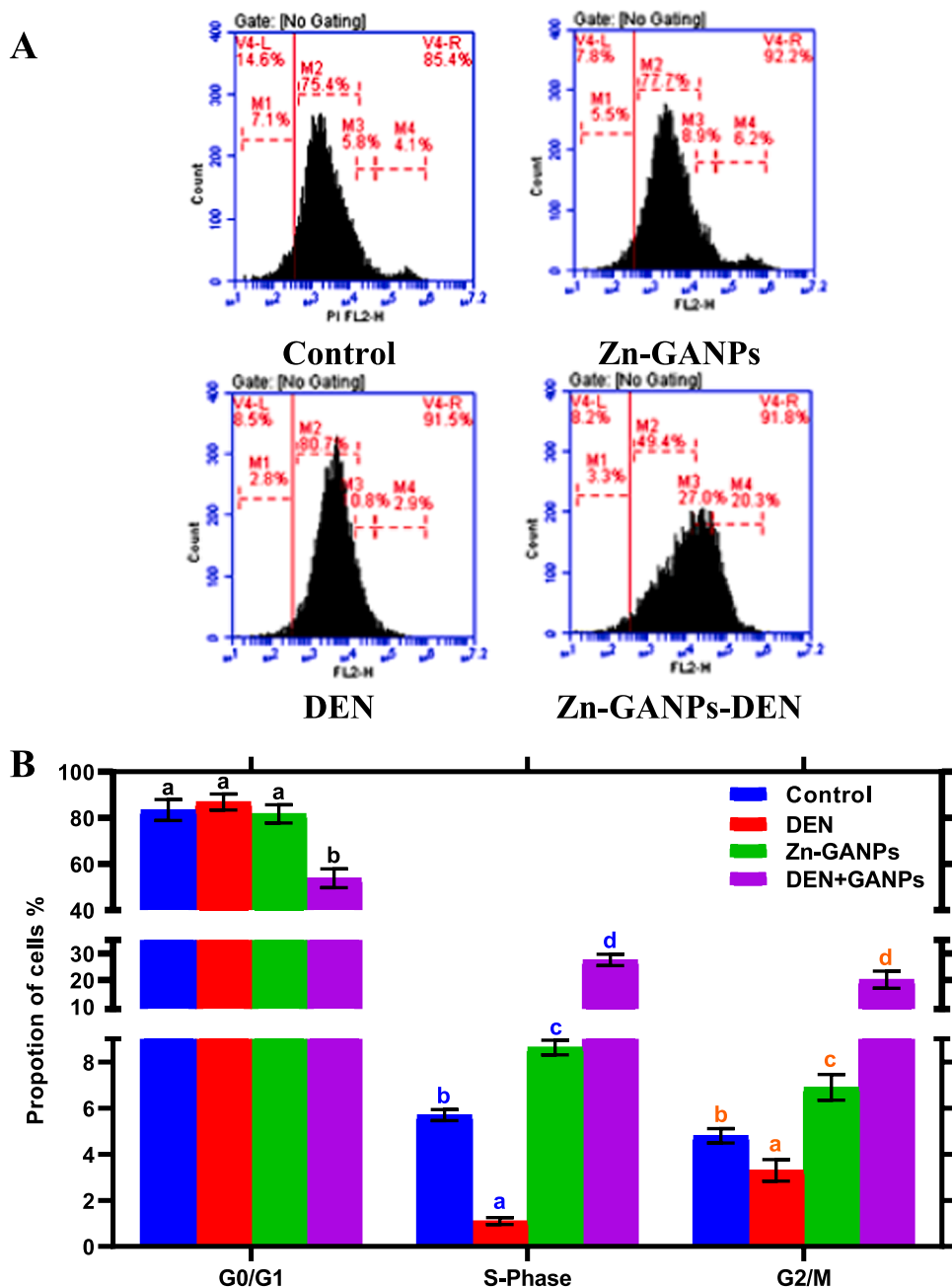


Fig. 8. Effect of Zn-GANPs on sub G0%, S phase G2M% and G1 apoptosis in liver tissue of different groups. (A) Flow cytometry of cell cycle phases (G0/G1, S and G2/M) distribution. (B) The percentage of each phase in the cell cycle. Each experiment was repeated three times, data are expressed as the mean \pm SD (n = 10). Columns carrying different letters are significantly different (one-way ANOVA) ($p < 0.05$).

peroxidase (GPX), glutathione S-transferase (GST), SOD, and CAT, as well as non-enzymatic vitamin C, α -tocopherol, and GSH, predominantly eliminate free oxygen radicals [69]. In many studies that looked at preventing HCC, rats that were given DEN had much lower levels of antioxidant enzymes and non-enzymatic antioxidants [23,63]. Antioxidant parameters may decrease owing to hepatocellular injury or excessive use in scavenging DEN metabolism-generated free radicals. It protects cells from ROS by decomposing extracellular and internal hydrogen peroxide (H_2O_2). Catalase is homotetrameric. Hepatocellular carcinoma and other malignancies reduce catalase expression [70]. In HCC cell lines, prolonged ROS exposure methylated CpG island II on the catalase promoter and downregulated transcriptional catalase expression [71]. Glutathione deficiency increases sensitivity to oxidative stress, which promotes cancer growth, whereas increasing GSH levels boosts

antioxidant capacity and resistance to oxidative stress in many cancer cells [72].

In this investigation, Zn-GANP therapy increased liver tissue CAT and GSH significantly compared to DEN. Gallic acid might lower the production of free radicals by changing the activities of cytochrome P450-dependent mono-oxygenase and increasing the activities of epoxide hydrolase [73]. Earlier studies have shown gallic acid's free radical scavenging [74]. Free radical-scavenging phenolic hydroxyl groups are also effective. GA's antioxidant effects may come from its three hydroxyl groups. Treating rats with GA dramatically restored CAT activity [75]. GSH and catalase levels increased with zinc therapy for liver damage [76]. Zn is an antioxidant in some chemical systems. Metallothionein (MT) induction protects sulfhydryl groups from oxidation in GSH and inhibits transition metal reactive oxygen generation

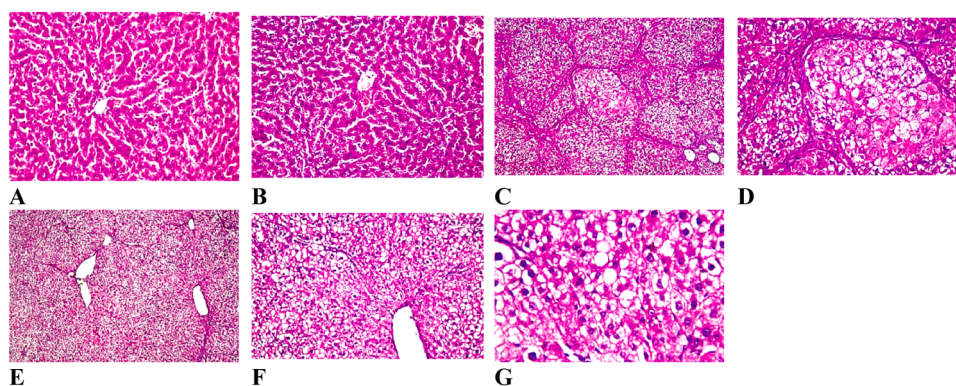


Fig. 9. A) Liver of rats in control group (H&E, x40). B) Liver of rats received Zn-GANPs at a dose of (20 mg/kg b.wt/day). C) Liver of rats received DEN 20 mg/kg b. wt (DEN H&E, x16). D) Liver of rats received DEN (H&E, x40). E) Liver of rats received DEN (20 mg/Kg b.wt) for 8 weeks and subsequently treated with Zn-GANPs (20 mg/kg b.wt/day) from the 9th week till the end of the experiment (13 weeks) (DEN- Zn-GANPs, H&E, x16). F) DEN-Zn-GANPs (H&E, x40). G) DEN- Zn-GANPs (H&E, x80).

[77], Zinc increases hepatocellular MT, which may help absorb, store, and detoxify trace metals such as zinc, copper, cadmium, mercury, and chromium [78].

The interaction between ROS and polyunsaturated fatty acids produces toxic and reactive aldehyde metabolites like L-MDA, which are the end products of lipid peroxidation. The significant cytotoxicity and protective enzyme inhibition of L-MDA imply it promotes tumor growth and co-carcinogenicity [79]. The well-known mutagen L-MDA interacts with deoxyguanosine to create a significant endogenous adduct in liver DNA [80]. DEN-induced liver cancer in rats had a significantly higher liver L-MDA concentration than the control normal group at the conclusion of the trial. Functional groups of numerous cellular components may interact with L-L-MDA to induce tumor development. Lipid peroxidation is linked to aging, heart disease, and cancer. In several investigations, primary and metastatic liver cancer patients had considerably greater blood L-MDA levels than the normal group. Due to increased ROS generation, liver cancer may cause substantial lipid peroxidation. L-MDA may oxidize protein amino acid residues and break them down. Deactivating selenium-dependent glutathione peroxidases may increase cellular glutathione consumption and oxidative stress [79].

Animals with DEN-induced liver cancer that were given Zn-GANPs had much lower levels of L-MDA in their livers than animals that were not given any treatment. Zn-GANPs may reduce oxidative stress by scavenging free radicals. Gallic acid and zinc may prevent and cure liver failure by reducing lipid peroxidation-mediated oxidative stress. Nanoparticles may boost cellular antioxidant enzyme production. DEN-injured animals' chemopreventive and antioxidant enzyme systems are restored by Gallic acid [81]. Zinc lowers plasma lipid peroxidation products and DNA adducts [82]. Zinc therapy corrected liver toxicity-induced lipid peroxidation [76].

4.5. Effect of Zn-GANPs on liver tissue TGF- β 1% and cell cycle analysis in normal and DEN-induced liver cancer

According to the latest findings, DEN-induced hepatocellular cancer had a significantly higher TGF-1 levels than the control. When compared to the DEN group, treatment with Zn-GANPs shown a substantial reduction in TGF-1 levels. According to Guo et al., exposure of murine photoreceptor-derived cells to ZnO NPs decreased the production of Matrix Metalloproteinase-9 (MMP-9) and TGF- β , which in turn impaired the ability of cells to proliferate and migrate. Reduced MMP-9 and TGF- β could not effectively activate signaling pathways involved in cell proliferation and migration, which decreased target cell proliferation and migration [83].

According to Chen et al., DEN treatment significantly increased TGF-

β 1 levels by around two times compared to the control group. In comparison to the DEN group, the levels of TGF-1 were considerably reduced after treatment with GA (50 and 100 mg/kg) or silymarin. TGF- β 1 levels were almost able to return to those of the control at the highest dosage of GA [84]. TGF- β is thought to have a key role in controlling liver carcinogenesis and promoting liver fibrosis. The TGF- β signal transduction pathway is mediated intracellularly by Smad2 and Smad3. GA can reduce DEN-induced acute liver damage in mice, pointing to a putative mechanism whereby raising glutathione-s-transferase alpha 3 (GSTA3) and hemeoxygenase-1 (HO-1) expressions and might improve the liver capacity to detoxify substances [85]. It also highlighted another potential mechanism by which GA could reverse the negative effects of DEN, namely the involvement of the crucial TGF- β /Smad pathway.

The results showed that, compared to the DEN group, the Zn-GANPs + DEN treated group had significantly less cells in G0/G1, more cells in S phase, and more cells in G2/M, which suggested Zn-GANPs-induced apoptosis, S phase, and G2/M cycle arrest. According to research, DNA damage often causes three biological reactions: cell death, an increase in DNA repair, and cell cycle arrest [86]. According to our findings, Zn-GANPs caused genotoxic stress, DNA strand breakage, and activation of RNA-activated Protein Kinase (PKR) and Bcl-2-Associated Death Promoter (BAD) signal transducers [87]. Zn-GANPs cause G2/M cell cycle arrest, which then limits DNA repair by preventing the growth of H2AX foci.

A number of kinases are activated in response to DNA damage and link the checkpoint to the cell cycle machinery. Cell cycle arrest can result from the DNA damage checkpoint's activation, which involves the activation of serine/threonine protein kinase or Ataxia-telangiectasia mutated (ATM) kinase and ATM autophosphorylation at Ser1981. This prevents mitosis in the presence of damaged DNA. Cancer cell growth is slowed down by G2/M phase arrest, and G2/M phase cells are more radiation-sensitive [88]. As a result, the G2/M transition is seen as a distinct target, and this arrest may be an effective CRT technique. One of the important proteins in checkpoint pathways is the tumor suppressor p53. Growth arrest in both the G1 and G2/M phases may result from the activation of p53. The promoter of the p21 cyclin-dependent kinase (Cdk) inhibitor is bound by overexpressed p53, which results in p21 accumulated in the conventional p53-dependent G2/M phase arrest pathway. Cell cycle arrest results from the ensuing suppression of cell division cycle 2 Cdc2-cyclin B1 activity. However, several investigations have shown that p53 deficit or mutation alone is sufficient to cause G2/M arrest, and in p53-deficient cells, this pathway switches from p21-dependent to checkpoint kinase Chk-dependent [89].

In comparison to control cells, Zn-GANPs treatment raised the G2/M phase, reduced the G0/G1 phase, and slightly increased the S phase, indicating that it triggers cell death in G0/G1 cells and causes a cell cycle

arrest in the G2/M phase. The downstream target p21 of p53 caused G2/M arrest [90]. This study investigated whether bcl-2-mediated cell cycle arrest may explain how Zn-GANPs consistently changed cell cycle progression. GA therapy substantially and dose-dependently slowed the proliferation of cancer cells, according to Hsu et al. Additional flow cytometric research revealed that GA significantly caused G2/M phase arrest [91].

Numerous investigations reported that ZnO-NPs treatment caused a deposition and observable peak at sub-G0/G1, which represents the population of apoptotic and dead cells [92]. Compared to untreated EC-bearing animals, there was a significant decrease in G0/G1, S phase, and G2/M populations, indicating a striking rise in the number of dead cells and cell cycle arrest in G0/G1 [93].

In order to damage mitochondria and release cytochrome c from those organelles into the cytosol, the pro-apoptotic Bax and Bak proteins must oligomerize. Tp53 directly inhibits the anti-apoptotic Bcl-2 and Bcl-XL proteins with promotes the mitochondria-dependent apoptotic pathway [94]. It is believed that the ratio of Bcl-2 to Bax, rather than the concentrations of individual proteins, is what determines whether a cell will survive or die [95]. In order to identify the mitochondria-mediated apoptotic pathway linked to the use of Zn-GANPs, bcl-2 and caspase-3 gene expression were examined [96].

5. Conclusion

In this study, liver carcinogenesis was initiated in Wistar rats by exposing them to Diethylnitrosamine (DEN). Subsequent histopathological analysis of the rat livers unveiled the degeneration of fibrous tissue strands that separate vascular structures, along with the occurrence of coagulative necrosis in hepatocytes within the parenchyma, leading to the disorganization of lobular structures in the sections from the DEN group. In contrast, the sections from the Zn-GANPs treated group exhibited improvements in these conditions, thereby validating the reliability of the experimental carcinogenesis model employed.

Oral administration of Zn-GANPs resulted in a reduction in the formation of the oxidative damage marker MDA, while increasing the catalase activity and GSH levels. Additionally, Zn-GANPs led to decreased liver function test indicators such as ALT, AST, GGT activities, and total bilirubin levels. Treatment with Zn-GANPs in rats demonstrated increased levels of total protein, albumin, globulin, and the A/G ratio. Furthermore, it reduced AFP, NF- κ B P65, and Bcl2 levels while elevating caspase-3 levels. The anti-inflammatory, antioxidant, and pro-apoptotic properties of Zn-GANPs in this study significantly improved both histological and biochemical outcomes in the context of DEN-induced liver carcinoma. Remarkably, Zn-GANPs induced cell cycle arrest during the S and G2/M phases and promoted apoptosis during the G0/G1 phase of DEN-induced liver carcinoma by upregulating caspase-3 and downregulating Bcl-2. These findings underscore Zn-GANPs as a promising adjunctive compound for inhibiting the progression of liver cancer. Nonetheless, further research is needed to elucidate the signaling pathways governing these processes, thus enhancing the therapeutic potential of Zn-GANPs across a range of cancer types.

CRedit authorship contribution statement

EL-sonbaty Sawsan M.: Software, Methodology, Investigation, Formal analysis, Data curation. **El-Tayeb Mohamed A.:** Validation, Software, Methodology, Formal analysis, Data curation. **Salem Maha A.:** Methodology, Investigation, Formal analysis, Data curation. **Shoker Faten E.:** Methodology, Investigation, Formal analysis, Data curation. **Emad Ayat M.:** Validation, Methodology, Investigation, Data curation. **Rao Arunagiri Kuha Deva Magendhra:** Validation, Software, Methodology, Formal analysis. **Mani Samson:** Validation, Software, Formal analysis, Data curation. **Kotob Mohamed H.:** Writing – review & editing, Visualization, Methodology, Investigation, Formal analysis, Data curation. **AboZaid Omayma A. R.:** Writing – original draft, Validation,

Software, Methodology, Investigation, Formal analysis, Data curation. **Mamdouh Mohamed A.:** Validation, Investigation, Formal analysis, Data curation. **Aufy Mohammed:** Writing – review & editing, Visualization, Validation, Supervision, Methodology, Formal analysis, Data curation, Conceptualization. **Saleh Ibrahim A.:** Validation, Software, Methodology, Investigation, Formal analysis. **Kodous Ahmad S.:** Writing – review & editing, Supervision, Project administration, Methodology, Formal analysis, Data curation, Conceptualization. **Abdel-Maksoud Mostafa A.:** Writing – review & editing, Software, Project administration, Methodology, Funding acquisition, Data curation.

Declaration of Competing Interest

The authors declare no conflict of interest.

Acknowledgement

The authors extend their appreciation to the Researchers Supporting Project number (RSPD2024R678) King Saud University, Riyadh, Saudi Arabia.

References

- [1] F. Bray, J. Ferlay, I. Soerjomataram, R.L. Siegel, L.A. Torre, A. Jemal, Global cancer statistics 2018: GLOBOCAN estimates of incidence and mortality worldwide for 36 cancers in 185 countries, *Ca. Cancer J. Clin.* 68 (2018) 394–424, <https://doi.org/10.3322/caac.21492>.
- [2] A. Desai, S. Sandhu, J.-P. Lai, D.S. Sandhu, Hepatocellular carcinoma in non-cirrhotic liver: a comprehensive review, *World J. Hepatol.* 11 (2019) 1–18, <https://doi.org/10.4254/wjh.v11.i1.1>.
- [3] N.Z. Shaban, S.A. Abdelrahman, M.A.L. El-Kersh, F.A.K. Mogahed, I.M. Talaat, N. H. Habashy, The synergistic hepatoprotective potential of Beta vulgaris juice and 2,3-dimercaptosuccinic acid in lead-intoxicated rats via improving the hepatic oxidative and inflammatory stress, *BMC Complement. Med. Ther.* 20 (2020), <https://doi.org/10.1186/s12906-020-03056-6>.
- [4] A.S. Kodous, M.M. Atta, G.R. Abdel-Hamid, H.A. Ashry, Anti-metastatic cancer activity of ultrasonic synthesized reduced graphene oxide/copper composites, *Chem. Pap.* (2021), <https://doi.org/10.1007/s11696-021-01866-7>.
- [5] B. Alshahrani, H.I. ElSaeedy, S. Fares, A.H. Korna, H.A. Yakout, A.H. Ashour, R. A. Fahim, A.S. Kodous, M. Gobara, M.I.A.A. Maksoud, Structural, optical, and magnetic properties of nanostructured Ag-substituted Co-Zn ferrites: insights on anticancer and antiproliferative activities, *J. Mater. Sci. Mater. Electron.* 32 (2021) 12383–12401, <https://doi.org/10.1007/s10854-021-05870-1>.
- [6] M.J. Akhtar, M. Ahamed, S. Kumar, M.M. Khan, J. Ahmad, S.A. Alrokayan, Zinc oxide nanoparticles selectively induce apoptosis in human cancer cells through reactive oxygen species, *Int. J. Nanomed.* 7 (2012) 845–857, <https://doi.org/10.2147/IJN.S29129>.
- [7] H.F.H. Hassan, A.M. Mansour, A.M.H. Abo-Youssef, B.E.M. Elsadek, B.A.S. Messiha, Zinc oxide nanoparticles as a novel anticancer approach; in vitro and in vivo evidence, *Clin. Exp. Pharmacol. Physiol.* 44 (2017), <https://doi.org/10.1111/1440-1681.12681>.
- [8] F.D. Urnov, E.J. Rebar, M.C. Holmes, H.S. Zhang, P.D. Gregory, Genome editing with engineered zinc finger nucleases, *Nat. Rev. Genet.* 11 (2010), <https://doi.org/10.1038/nrg2842>.
- [9] K.R. Wessells, G.M. Singh, K.H. Brown, Estimating the global prevalence of inadequate zinc intake from national food balance sheets: effects of methodological assumptions, *PLoS One* 7 (2012), <https://doi.org/10.1371/journal.pone.0050565>.
- [10] D. Skrajnowska, B. Bobrowska-Korcak, Role of zinc in immune system and anticancer defense mechanisms, *Nutrients* 11 (2019), <https://doi.org/10.3390/nu11102273>.
- [11] D.K. Dhawan, V.D. Chadha, Zinc: A promising agent in dietary chemoprevention of cancer, *Indian J. Med. Res.* 132 (2010).
- [12] W. Elfalleh, Total phenolic contents and antioxidant activities of pomegranate peel, seed, leaf and flower, *J. Med. Plants Res.* 6 (2012), <https://doi.org/10.5897/jmpr11.995>.
- [13] N.Z. Shaban, M.A.L. El-Kersh, F.H. El-Rashidy, N.H. Habashy, Protective role of Punica granatum (pomegranate) peel and seed oil extracts on diethylnitrosamine and phenobarbital-induced hepatic injury in male rats, *Food Chem.* 141 (2013), <https://doi.org/10.1016/j.foodchem.2013.04.134>.
- [14] D. Dorniani, M.Z. Bin Hussein, A.U. Kura, S. Fakurazi, A.H. Shaari, Z. Ahmad, Preparation of Fe₃O₄ magnetic nanoparticles coated with gallic acid for drug delivery, *Int. J. Nanomed.* 7 (2012) 5745–5756, <https://doi.org/10.2147/IJN.S35746>.
- [15] M. Ashrafzadeh, A. Zarrabi, S. Mirzaei, F. Hashemi, S. Samarghandian, A. Zabolian, K. Hushmandi, H.L. Ang, G. Sethi, A.P. Kumar, K.S. Ahn, N. Nabavi, H. Khan, P. Makvandi, R.S. Varma, Gallic acid for cancer therapy: molecular mechanisms and boosting efficacy by nanospecific delivery, *Food Chem. Toxicol.* 157 (2021), <https://doi.org/10.1016/j.fct.2021.112576>.

- [16] S. Jones-Bolin, Guidelines for the care and use of laboratory animals in biomedical research, *Curr. Protoc. Pharmacol.* (2012), <https://doi.org/10.1002/0471141755.pha04bs59>.
- [17] A.M. Emad, S.F. Ali, M.R. Meselhy, E.A. Sattar, Comparative antioxidant activities of selected apiaceous plants using EPR technique, *Pharmacogn. J.* 11 (2019), <https://doi.org/10.5530/pj.2019.11.210>.
- [18] R. Chhillar, D. Dhingra, Antidepressant-like activity of gallic acid in mice subjected to unpredictable chronic mild stress, *Fundam. Clin. Pharmacol.* 27 (2013) 409–418, <https://doi.org/10.1111/j.1472-8206.2012.01040.x>.
- [19] H.A. Darwish, N.A. El-Boghady, Possible involvement of oxidative stress in diethylnitrosamine-induced hepatocarcinogenesis: chemopreventive effect of curcumin, *J. Food Biochem.* 37 (2013) 353–361, <https://doi.org/10.1111/j.1745-4514.2011.00637.x>.
- [20] H.U. Bergmeyer, M. Horder, R. Rej, International Federation of Clinical Chemistry (IFCC) Scientific Committee, Analytical Section: approved recommendation (1985) on IFCC methods for the measurement of catalytic concentration of enzymes, Part 3. IFCC Method alanine aminotransferase (L₇), *J. Clin. Chem. Clin. Biochem. Z. Fur Klin. Chem. Und Klin. Biochem.* 24 (1986) 481–495.
- [21] G. Szasz, A kinetic photometric method for serum γ -glutamyl transpeptidase, *Clin. Chem.* 15 (1969) 124–136, <https://doi.org/10.1093/clinchem/15.2.124>.
- [22] G.R. Kingsley, The determination of serum total protein, albumin, and globulin by the biuret reaction, *J. Biol. Chem.* 131 (1939) 197–200, [https://doi.org/10.1016/S0021-9258\(18\)73494-7](https://doi.org/10.1016/S0021-9258(18)73494-7).
- [23] Y.R. Shahin, N.M. Elguindy, A. Abdel Bary, M. Balbaa, The protective mechanism of *Nigella sativa* against diethylnitrosamine-induced hepatocellular carcinoma through its antioxidant effect and EGFR/ERK1/2 signaling, *Environ. Toxicol.* 33 (2018) 885–898, <https://doi.org/10.1002/tox.22574>.
- [24] H.B.T.-M. in E. Aebi, [13] Catalase in vitro, in: *Oxyg. Radicals Biol. Syst.*, Academic Press, 1984; pp. 121–126. [https://doi.org/https://doi.org/10.1016/S0076-6879\(84\)05016-3](https://doi.org/https://doi.org/10.1016/S0076-6879(84)05016-3).
- [25] M.S. Moron, J.W. Depierre, B. Mannervik, Levels of glutathione, glutathione reductase and glutathione S-transferase activities in rat lung and liver, *Biochim. Biophys. Acta - Gen. Subj.* 582 (1979) 67–78, [https://doi.org/10.1016/0304-4165\(79\)90289-7](https://doi.org/10.1016/0304-4165(79)90289-7).
- [26] H. Ohkawa, N. Ohishi, K. Yagi, Assay for lipid peroxides in animal tissues by thiobarbituric acid reaction, *Anal. Biochem.* 95 (1979) 351–358, [https://doi.org/10.1016/0003-2697\(79\)90738-3](https://doi.org/10.1016/0003-2697(79)90738-3).
- [27] T. Heiden, J. Castro, B.M. Graf, B. Tribukait, Comparison of routine flow cytometric DNA analysis of fresh tissues in two laboratories: effects of differences in preparation methods and background models of cell cycle calculation, *Commun. Clin. Cytom.* 34 (1998) 187–197, [https://doi.org/10.1002/\(SICI\)1097-0320\(19980815\)34:4<187::AID-CYTO3>3.0.CO;2-D](https://doi.org/10.1002/(SICI)1097-0320(19980815)34:4<187::AID-CYTO3>3.0.CO;2-D).
- [28] F. Spyrtatos, DNA content and cell cycle analysis by flow cytometry in clinical samples: application in breast cancer, *Biol. Cell.* 78 (1993), [https://doi.org/10.1016/0248-4900\(93\)90116-V](https://doi.org/10.1016/0248-4900(93)90116-V).
- [29] D.R. Bancroft, J.D., Stevens, A., & Turner, Theory and practice of histological techniques, 4th ed., Churchill Livingstone, New York, London, San Francisco, Tokyo, 1996.
- [30] M.L. Swift, GraphPad prism, Data analysis, and scientific graphing, *J. Chem. Inf. Comput. Sci.* 37 (1997) 411–412, <https://doi.org/10.1021/ci960402j>.
- [31] N. Shang, T. Bank, X. Ding, P. Breslin, J. Li, B. Shi, W. Qiu, Caspase-3 suppresses diethylnitrosamine-induced hepatocyte death, compensatory proliferation and hepatocarcinogenesis through inhibiting p38 activation, *Cell Death Dis.* 9 (2018) 558, <https://doi.org/10.1038/s41419-018-0617-7>.
- [32] P. Rana, G. Soni, Antioxidant potential of thyme extract: alleviation of N-nitrosodiethylamine-induced oxidative stress, *Hum. Exp. Toxicol.* 27 (2008) 215–221, <https://doi.org/10.1177/0960327108088970>.
- [33] Y.Y. Lee, J.-M. Galano, H.H. Leung, L. Balas, C. Oger, T. Durand, J.C.-Y. Lee, Nonenzymatic oxygenated metabolite of docosahexaenoic acid, 4(RS)-4-F4t-neuroprostane, acts as a bioactive lipid molecule in neuronal cells, *FEBS Lett.* 594 (2020) 1797–1808, <https://doi.org/10.1002/1873-3468.13774>.
- [34] F.P. Guengerich, Cytochrome P450 2E1 and its roles in disease, *Chem. Biol. Interact.* 322 (2020) 109056, <https://doi.org/10.1016/j.cbi.2020.109056>.
- [35] H. Bartsch, E. Hietanen, C. Malaveille, Carcinogenic nitrosamines: free radical aspects of their action, *Free Radic. Biol. Med.* 7 (1989) 637–644, [https://doi.org/10.1016/0891-5849\(89\)90144-5](https://doi.org/10.1016/0891-5849(89)90144-5).
- [36] J. Yeong, A.A. Thike, M. Ikeda, J.C.T. Lim, B. Lee, S. Nakamura, J. Iqbal, P.H. Tan, Caveolin-1 expression as a prognostic marker in triple negative breast cancers of Asian women, *J. Clin. Pathol.* 71 (2018), <https://doi.org/10.1136/jclinpath-2017-204495>.
- [37] N. González-Abuín, N. Martínez-Micaelo, M. Margalef, M. Blay, A. Arola-Arnal, B. Guquerza, A. Ardevol, M. Pinent, A grape seed extract increases active glucagon-like peptide-1 levels after an oral glucose load in rats, *Food Funct.* 5 (2014) 2357–2364, <https://doi.org/10.1039/c4fo00447g>.
- [38] D.H. Assar, A.A.A. Mokhatbaty, E.W. Ghazy, A.E. Ragab, S.A. Asa, W. Abdo, Z. I. Elbially, N.E. Mohamed, A.H. El-Far, Ameliorative effects of aspergillus awamori against the initiation of hepatocarcinogenesis induced by diethylnitrosamine in a rat model: regulation of cyp19 and p53 gene expression, *Antioxidants* 10 (2021), <https://doi.org/10.3390/antiox10060922>.
- [39] R. Sallie, J. Michael Tredger, R. Williams, Drugs and the liver part 1: testing liver function, *Biopharm. \ Drug Dispos.* 12 (1991) 251–259, <https://doi.org/10.1002/bdd.2510120403>.
- [40] M.R. McGill, The past and present of serum aminotransferases and the future of liver injury biomarkers, *EXCLI J.* 15 (2016) 817–828, <https://doi.org/10.17197/excli2016-800>.
- [41] C.-H. Yang, H.-Y. Chang, Y.-C. Chen, C.-C. Lu, S.-S. Huang, G.-J. Huang, H.-C. Lai, Ethanol extract of *Phellinus merrillii* protects against diethylnitrosamine- and 2-acetylaminofluorene-induced hepatocarcinogenesis in rats, *Chin. J. Integr. Med.* 23 (2017) 117–124, <https://doi.org/10.1007/s11655-016-2513-2>.
- [42] D.M. Kopustinskiene, V. Jakstas, A. Savickas, J. Bernatoniene, Flavonoids as anticancer agents, *Nutrients* 12 (2020), <https://doi.org/10.3390/nu12020457>.
- [43] N.M. El-Lakkany, W.H. El-Maadawy, S.H. Seif el-Din, S. Saleh, M.M. Safar, S. M. Ezzat, S.H. Mohamed, S.S. Botros, Z. Demerdash, O.A. Hammam, Antifibrotic effects of gallic acid on hepatic stellate cells: In vitro and in vivo mechanistic study, *J. Tradit. Complement. Med.* 9 (2019) 45–53, <https://doi.org/10.1016/j.jtcm.2018.01.010>.
- [44] S.A. Gani, S.A. Muhammad, A.U. Kura, F. Barahua, M.Z. Hussein, S. Fakurazi, Effect of protocatechuic acid-layered double hydroxide nanoparticles on diethylnitrosamine/phenobarbital-induced hepatocellular carcinoma in mice, *PLoS One* 14 (2019) e0217009, <https://doi.org/10.1371/journal.pone.0217009>.
- [45] B.I. Carr, V. Guerra, E.G. Giannini, F. Farinati, F. Ciccarese, G. Ludovico Rapaccini, M. Di Marco, L. Benvenuto, M. Zoli, F. Borzio, E. Caturelli, M. Chiaramonte, F. Trevisani, Association of abnormal plasma bilirubin with aggressive hepatocellular carcinoma phenotype, *Semin. Oncol.* 41 (2014) 252–258, <https://doi.org/10.1053/j.seminoncol.2014.03.006>.
- [46] B. Raj Kapoor, B. Jayakar, N. Muruges, D. Sakthisekaran, Chemoprevention and cytotoxic effect of *Bauhinia variegata* against N-nitrosodiethylamine induced liver tumors and human cancer cell lines, *J. Ethnopharmacol.* 104 (2006) 407–409, <https://doi.org/10.1016/j.jep.2005.08.074>.
- [47] X. Jin, T. Zhao, D. Shi, M.B. Ye, Q. Yi, Protective role of fucoxanthin in diethylnitrosamine-induced hepatocarcinogenesis in experimental adult rats, *Drug Dev. Res.* 80 (2019) 209–217, <https://doi.org/10.1002/ddr.21451>.
- [48] G. Akbari, F. Savari, S.A. Mard, A. Rezaie, M. Moradi, Gallic acid protects the liver in rats against injuries induced by transient ischemia-reperfusion through regulating microRNAs expressions, *Iran. J. Basic Med. Sci.* 22 (2019) 439–444, <https://doi.org/10.22038/ijbms.2018.31589.7605>.
- [49] F. Aiad, B. El-Gamal, J. Al-Meer, Z. El-Kerdasy, N. Zakhary, A. El-Aaser, Protective effect of soybean against hepatocarcinogenesis induced by DL-ethionine, *J. Biochem. Mol. Biol.* 37 (2004) 370–375, <https://doi.org/10.5483/bmbrep.2004.37.3.370>.
- [50] G. Di Stefano, C. Busi, L. Fiume, Fluoridation coupling with lactosaminated human albumin to increase drug efficacy on liver micrometastases, *Dig. Liver Dis.* 34 (2002) 439–446, [https://doi.org/10.1016/S1590-8658\(02\)80042-1](https://doi.org/10.1016/S1590-8658(02)80042-1).
- [51] V.W.-S. Wong, S.L. Chan, F. Mo, T.-C. Chan, H.H.-F. Loong, G.L.-H. Wong, Y.Y.-N. Lui, A.T.-C. Chan, J.J.-Y. Sung, W. Yeo, H.L.-Y. Chan, T.S.-K. Mok, Clinical scoring system to predict hepatocellular carcinoma in chronic hepatitis B carriers, *J. Clin. Oncol. \ J. Am. Soc. Clin. Oncol.* 28 (2010) 1660–1665, <https://doi.org/10.1200/JCO.2009.26.2675>.
- [52] A. Abbasi, A.R. Bhutto, N. Butt, S.M. Munir, Correlation of serum alpha fetoprotein and tumor size in hepatocellular carcinoma, *J. Pak. Med. Assoc.* 62 (2012) 33–36.
- [53] C.E. Cross, B. Halliwell, E.T. Borish, W.A. Pryor, B.N. Ames, R.L. Saul, J. M. McCord, D. Harman, Oxygen radicals and human disease, *Ann. Intern. Med.* 107 (1987) 526–545, <https://doi.org/10.7326/0003-4819-107-4-526>.
- [54] R. Kikkawa, M. Fujikawa, T. Yamamoto, Y. Hamada, H. Yamada, I. Horii, In vivo hepatotoxicity study of rats in comparison with in vitro hepatotoxicity screening system, *J. Toxicol. Sci.* 31 (2006) 23–34, <https://doi.org/10.2131/jts.31.23>.
- [55] R.S. Tupe, S.G. Tupe, K.V. Tarwadi, V.V. Agte, Effect of different dietary zinc levels on hepatic antioxidant and micronutrients indices under oxidative stress conditions, *Metabolism* 59 (2010) 1603–1611, <https://doi.org/10.1016/j.metabol.2010.02.020>.
- [56] T. Marino, A. Galano, N. Russo, Radical scavenging ability of gallic acid toward OH and OOH radicals. Reaction mechanism and rate constants from the density functional Theory, *J. Phys. Chem. B.* 118 (2014) 10380–10389, <https://doi.org/10.1021/jp505589b>.
- [57] D.G. Ahn, H.J. Kim, H. Kang, H.W. Lee, S.H. Bae, J.H. Lee, Y.H. Paik, J.S. Lee, Feasibility of α -fetoprotein as a diagnostic tool for hepatocellular carcinoma in Korea, *Korean J. Intern. Med.* 31 (2016) 46–53, <https://doi.org/10.3904/kjim.2016.31.1.46>.
- [58] P.N. Alexandrov, Y. Zhao, B.M. Jones, S. Bhattacharjee, W.J. Lukiw, Expression of the phagocytosis-essential protein TREM2 is down-regulated by an aluminum-induced miRNA-34a in a murine microglial cell line, *J. Inorg. Biochem.* 128 (2013) 267–269, <https://doi.org/10.1016/j.jinorgbio.2013.05.010>.
- [59] O. Karimi-Khouzani, E. Heidarian, S.A. Amini, Anti-inflammatory and ameliorative effects of gallic acid on fluoxetine-induced oxidative stress and liver damage in rats, *Pharmacol. Rep.* 69 (2017) 830–835, <https://doi.org/10.1016/j.pharep.2017.03.011>.
- [60] G. Sun, S. Zhang, Y. Xie, Z. Zhang, W. Zhao, Gallic acid as a selective anticancer agent that induces apoptosis in SMMC-7721 human hepatocellular carcinoma cells, *Oncol. Lett.* 11 (2016) 150–158, <https://doi.org/10.3892/ol.2015.3845>.
- [61] T. Luedde, R.F. Schwabe, NF- κ B in the liver—linking injury, fibrosis and hepatocellular carcinoma, *Nat. Rev. Gastroenterol. Hepatol.* 8 (2011) 108–118, <https://doi.org/10.1038/nrgastro.2010.213>.
- [62] B.H. O'Neil, P. Bůžková, H. Farrah, D. Kashatus, H. Sanoff, R.M. Goldberg, A. S. Baldwin, W.K. Funkhouser, Expression of nuclear factor-kappaB family proteins in hepatocellular carcinomas, *Oncology* 72 (2007) 97–104, <https://doi.org/10.1159/000111116>.
- [63] L. Wan, J. Shen, Y. Wang, W. Zhao, N. Fang, X. Yuan, B. Xue, Extracts of *Qizhu* decoction inhibit hepatitis and hepatocellular carcinoma in vitro and in C57BL/6 mice by suppressing NF- κ B signaling, *Sci. Rep.* 9 (2019) 1415, <https://doi.org/10.1038/s41598-018-38391-9>.

- [64] L. Zhu, P. Gu, H. Shen, Gallic acid improved inflammation via NF- κ B pathway in TNBS-induced ulcerative colitis, *Int. Immunopharmacol.* 67 (2019) 129–137, <https://doi.org/10.1016/j.intimp.2018.11.049>.
- [65] B. Bao, A. Thakur, Y. Li, A. Ahmad, A.S. Azmi, S. Banerjee, D. Kong, S. Ali, L. G. Lum, F.H. Sarkar, The immunological contribution of NF- κ B within the tumor microenvironment: a potential protective role of zinc as an anti-tumor agent, *Biochim. Biophys. Acta - Rev. Cancer* 1825 (2012) 160–172, <https://doi.org/10.1016/j.bbcan.2011.11.002>.
- [66] S. Ma, G.G. Chen, P.B.S. Lai, Bcl-2 Family Members in Hepatocellular Carcinoma (HCC) – Mechanisms and Therapeutic Potentials, in: G.G. Chen, P.B.S. Lai (Eds.), *Apoptosis Carcinog. Chemother. Apoptosis Cancer*, Springer Netherlands, Dordrecht, 2009, pp. 219–235, https://doi.org/10.1007/978-1-4020-9597-9_9.
- [67] M.K. Kang, N.J. Kang, Y.J. Jang, K.W. Lee, H.J. Lee, Gallic acid induces neuronal cell death through activation of c-Jun N-terminal kinase and downregulation of Bcl-2, *Ann. N. Y. Acad. Sci.* 1171 (2009) 514–520, <https://doi.org/10.1111/j.1749-6632.2009.04728.x>.
- [68] J.H. Ku, S.Y. Seo, C. Kwak, H.H. Kim, The role of survivin and Bcl-2 in zinc-induced apoptosis in prostate cancer cells, *Urol. Oncol. Semin. Orig. Investig.* 30 (2012) 562–568, <https://doi.org/10.1016/j.urolonc.2010.06.001>.
- [69] S. Jayakumar, A. Madankumar, S. Asokkumar, S. Raghunandhakumar, K. Gokula dhas, S. Kamaraj, M.G. Josephine Divya, T. Devaki, Potential preventive effect of carvedilol against diethylnitrosamine-induced hepatocellular carcinoma in rats, *Mol. Cell. Biochem.* 360 (2012) 51–60, <https://doi.org/10.1007/s11010-011-1043-7>.
- [70] J.Y. Min, S.O. Lim, G. Jung, Downregulation of catalase by reactive oxygen species via hypermethylation of CpG island II on the catalase promoter, *FEBS Lett.* 584 (2010) 2427–2432, <https://doi.org/10.1016/j.febslet.2010.04.048>.
- [71] M.Y. Cho, J.Y. Cheong, W. Lim, S. Jo, Y. Lee, H.J. Wang, K.H. Han, H. Cho, Prognostic significance of catalase expression and its regulatory effects on hepatitis B virus X protein (HBx) in HBV-related advanced hepatocellular carcinomas, *Oncotarget* 5 (2014) 12233–12246, <https://doi.org/10.18632/oncotarget.2625>.
- [72] N. Traverso, R. Ricciarelli, M. Nitti, B. Marengo, A.L. Furfaro, M.A. Pronzato, U. M. Marinari, C. Domenicotti, Role of glutathione in cancer progression and chemoresistance, *Oxid. Med. Cell. Longev.* 2013 (2013) 972913, <https://doi.org/10.1155/2013/972913>.
- [73] D.K.P. Hau, R. Gambari, R.S.M. Wong, M.C.W. Yuen, G.Y.M. Cheng, C.S.W. Tong, G.Y. Zhu, A.K.M. Leung, P.B.S. Lai, F.Y. Lau, A.K.W. Chan, W.Y. Wong, S.H.L. Kok, C.H. Cheng, C.W. Kan, A.S.C. Chan, C.H. Chui, J.C.O. Tang, D.W.F. Fong, Phyllanthus urinaria extract attenuates acetaminophen induced hepatotoxicity: involvement of cytochrome P450 CYP2E1, *Phytomedicine* 16 (2009) 751–760, <https://doi.org/10.1016/j.phymed.2009.01.008>.
- [74] Y.J. Kim, Antimelanogenic and antioxidant properties of gallic acid, *Biol. Pharm. Bull.* 30 (2007) 1052–1055, <https://doi.org/10.1248/bpb.30.1052>.
- [75] J.S. Giftson, S. Jayanthi, N. Nalini, Chemopreventive efficacy of gallic acid, an antioxidant and anticarcinogenic polyphenol, against 1,2-dimethyl hydrazine induced rat colon carcinogenesis, *Invest. N. Drugs* 28 (2010) 251–259, <https://doi.org/10.1007/s10637-009-9241-9>.
- [76] A. Goel, V. Dani, D.K. Dhawan, Protective effects of zinc on lipid peroxidation, antioxidant enzymes and hepatic histoarchitecture in chlorpyrifos-induced toxicity, *Chem. Biol. Interact.* 156 (2005) 131–140, <https://doi.org/10.1016/j.cbi.2005.08.004>.
- [77] S.R. Lee, Critical role of zinc as either an antioxidant or a prooxidant in cellular systems, *Oxid. Med. Cell. Longev.* 2018 (2018) 9156285, <https://doi.org/10.1155/2018/9156285>.
- [78] M. Jarosz, M. Olbert, G. Wyszogrodzka, K. Mlyniec, T. Librowski, Antioxidant and anti-inflammatory effects of zinc. Zinc-dependent NF- κ B signaling, *Inflammopharmacology* 25 (2017) 11–24, <https://doi.org/10.1007/s10787-017-0309-4>.
- [79] A. Shirazi, E. Mihandoost, G. Ghobadi, M. Mohseni, M. Ghazi-Khansari, Evaluation of radio-protective effect of melatonin on whole body irradiation induced liver tissue damage, *Cell J.* 14 (2013) 292–297.
- [80] L.J. Marnett, Lipid peroxidation—DNA damage by malondialdehyde, *Mutat. Res. Mol. Mech. Mutagen.* 424 (1999) 83–95, [https://doi.org/10.1016/S0027-5107\(99\)00010-X](https://doi.org/10.1016/S0027-5107(99)00010-X).
- [81] N. Sangeetha, P. Viswanathan, T. Balasubramanian, N. Nalini, Colon cancer chemopreventive efficacy of silibinin through perturbation of xenobiotic metabolizing enzymes in experimental rats, *Eur. J. Pharmacol.* 674 (2012) 430–438, <https://doi.org/10.1016/j.ejphar.2011.11.008>.
- [82] A.S. Prasad, B. Bao, F.W.J. Beck, O. Kucuk, F.H. Sarkar, Antioxidant effect of zinc in humans, *Free Radic. Biol. Med.* 37 (2004) 1182–1190, <https://doi.org/10.1016/j.freeradbiomed.2004.07.007>.
- [83] D.D. Guo, Q.N. Li, C.M. Li, H.S. Bi, Zinc oxide nanoparticles inhibit murine photoreceptor-derived cell proliferation and migration via reducing TGF- β and MMP-9 expression in vitro, *Cell Prolif.* 48 (2015) 198, <https://doi.org/10.1111/CPR.12163>.
- [84] Y. Chen, Z. Zhou, Q. Mo, G. Zhou, Y. Wang, Gallic Acid Attenuates Dimethylnitrosamine-Induced Liver Fibrosis by Alteration of Smad Phosphoisoform Signaling in Rats, *Biomed. Res. Int.* 2018 (2018), <https://doi.org/10.1155/2018/1682743>.
- [85] S. Ma, Gallic acid attenuates dimethylnitrosamine-induced acute liver injury in mice through Nrf2-mediated induction of heme oxygenase-1 and glutathione-S-transferase Alpha 3, *Med. Chem. (Los. Angel.)* 4 (2014), <https://doi.org/10.4172/2161-0444.1000208>.
- [86] C.J. Norbury, I.D. Hickson, Cellular responses to DNA damage, *Annu. Rev. Pharmacol. Toxicol.* 41 (2001), <https://doi.org/10.1146/annurev.pharmtox.41.1.367>.
- [87] T.A. Zykova, F. Zhu, Y. Zhang, A.M. Bode, Z. Dong, Involvement of ERKs, RSK2 and PKR in UVA-induced signal transduction toward phosphorylation of E1F2 α (Ser51), *Carcinogenesis* 28 (2007), <https://doi.org/10.1093/carcin/bgm070>.
- [88] T.M. Pawlik, K. Keyomarsi, Role of cell cycle in mediating sensitivity to radiotherapy, *Int. J. Radiat. Oncol. Biol. Phys.* 59 (2004), <https://doi.org/10.1016/j.ijrobp.2004.03.005>.
- [89] H.J. Jo, J.D. Song, K.M. Kim, Y.H. Cho, K.H. Kim, Y.C. Park, Diallyl disulfide induces reversible G2/M phase arrest on a p53-independent mechanism in human colon cancer HCT-116 cells, *Oncol. Rep.* 19 (2008), <https://doi.org/10.3892/or.19.1.275>.
- [90] H.F. Lu, Y.S. Chen, J.S. Yang, J.C. Chen, K.W. Lu, T.H. Chiu, K.C. Liu, C.C. Yeh, G. W. Chen, H.J. Lin, J.G. Chung, Gypenosides induced G0/G1 arrest via inhibition of cyclin E and induction of apoptosis via activation of caspases-3 and -9 in human lung cancer A-549 cells, *Vivo (Brooklyn)* 22 (2008).
- [91] J.D. Hsu, S.H. Kao, T.T. Ou, Y.J. Chen, Y.J. Li, C.J. Wang, Gallic acid induces G2/M phase arrest of breast cancer cell MCF-7 through stabilization of p27Kip1 attributed to disruption of p27Kip1/Skp2 complex, *J. Agric. Food Chem.* 59 (2011) 1996–2003, <https://doi.org/10.1021/JF103656V>.
- [92] M.F. Sanad, N.S. G. MA, A lot of promise for ZnO-5FU nanoparticles cytotoxicity against breast cancer cell lines, *J. Nanomed. Nanotechnol.* 09 (2018), <https://doi.org/10.4172/2157-7439.1000486>.
- [93] H.M. Sayed, M.M. Said, N.Y.S. Morcos, M.A. El Gawish, A.F.M. Ismail, Antitumor and Radiosensitizing Effects of Zinc Oxide-Caffeic Acid Nanoparticles against Solid Ehrlich Carcinoma in Female Mice, <https://doi.org/10.1177/15347354211021920>.
- [94] D. Tomas, [Apoptosis, UV-radiation, precancerosis and skin tumors], *Acta Med. Croat.* 63 (Suppl 2) (2009) 53–58.
- [95] Z.N. Oltval, C.L. Milliman, S.J. Korsmeyer, Bcl-2 heterodimerizes in vivo with a conserved homolog, Bax, that accelerates programmed cell death, *Cell* 74 (1993), [https://doi.org/10.1016/0092-8674\(93\)90509-0](https://doi.org/10.1016/0092-8674(93)90509-0).
- [96] H.S. Choi, M.C. Cho, H.G. Lee, D.Y. Yoon, Indole-3-carbinol induces apoptosis through p53 and activation of caspase-8 pathway in lung cancer A549 cells, *Food Chem. Toxicol.* 48 (2010) 883–890, <https://doi.org/10.1016/j.fct.2009.12.028>.